

Amphiboles in Andesite and Basalt: I. Stability as a Function of P - T - f_{O_2}

J. C. ALLEN,

*Department of Geology and Geography, Bucknell University
Lewisburg, Pennsylvania 17837*

A. L. BOETTCHER,

*Department of Geosciences, The Pennsylvania State University
University Park, Pennsylvania 16802*

AND G. MARLAND

*Department of Geography and Geology, Indiana State University
Terre Haute, Indiana 47809*

Abstract

The stabilities of amphiboles have been determined in an andesite, three basalts, and an olivine nephelinite in the presence of H_2O vapor at values of oxygen fugacity approximating those of Fe_3O_4 - Fe_2O_3 , Ni - NiO , and Fe_3O_4 - FeO . The thermal stability decreases with increasing activity of silica in the parent rocks. Maximum thermal stability of amphibole occurs at $1090^\circ C$ at 13 kbar in the Hualalai alkali basalt. Maximum pressure stability occurs at 31.5 kbar at a temperature of $1030^\circ C$ in the olivine nephelinite. Amphibole-bearing assemblages convert to garnet-bearing assemblages at pressures above 18 to 30 kbar. The amphiboles straddle the calciferous-subcalciferous boundary, and all of them fall in the pargasite-tschermakite-tschermakitic hornblende category. No orthopyroxene was found in any of the basaltic compositions under any of the conditions investigated, although it did occur in the andesite. This restricts the potential P - T - X conditions under which fractional crystallization of orthopyroxene is an important mechanism in the derivation of SiO_2 -undersaturated magmas.

Our results are consistent with those hypotheses in which some andesitic magmas derive from basaltic compositions through amphibole-liquid equilibria. Fractionation of alkalis by amphiboles may contribute to the proposed gradient in K_2O across subduction zones at island arcs and continental margins. The shallow dips and depths of subducting slabs beneath orogenic-zone volcanoes is in concert with this model.

Introduction

Knowledge of the P - T conditions under which hydrous minerals, such as amphiboles, exist is fundamental to our understanding of melting and related processes in the crust-mantle system. As is well known, water dissolves in silicate liquids under pressure and lowers the temperature of the beginning of melting. If all of the water is bound in amphiboles or other hydrous phases, the chemical potential of water would be less than if the water were present as a nearly pure aqueous fluid, and temperatures of the beginning of melting would be higher (Burnham, 1967).

In addition, the K_2O contents and K_2O/Na_2O of

igneous rocks may increase continentward from the oceans, and the fractionation of alkali-bearing minerals, such as amphibole, at depths may play a role in this postulated trend. Fractionation of such amphiboles from a basaltic magma may give rise to andesitic magmas as proposed by Bowen (1928) and others.

To solve these problems, we experimentally established the stability of amphiboles in an andesite, three basalts, and an olivine nephelinite in the presence of H_2O vapor at values of oxygen fugacity (f_{O_2}) approximating those of Fe_3O_4 - Fe_2O_3 , Ni - NiO , and Fe_3O_4 - FeO , from 10 to 36 kbar, determining the pressures at which amphibole-bearing assemblages

transform to garnet-bearing assemblages, *i.e.*, at depths (<75–100 km) in the Earth.

Experimental Methods

Starting Materials

Starting mixes were prepared from a Mt. Hood andesite, a quartz-normative Picture Gorge tholeiite, a 1921 Kilauea olivine tholeiite, a nepheline-normative prehistoric Hualalai alkali basalt, and a Honolulu olivine nephelinite (Table 1). These rocks were chosen because they encompass a wide range of SiO₂ and alkali concentrations, and experimental work had previously been accomplished on some of these rocks at other conditions (Eggler, 1970, 1973; Hill and Boettcher, 1970; Holloway, 1970, 1971; Holloway and Burnham, 1969, 1972; Yoder and Tilley, 1962; Fudali, 1965; Tuthill, 1968). All samples were crushed to –200 mesh under acetone, dried in an oven at 110°C, and stored in sealed vials over KOH in a dessicator.

Capsules

Because the T - f_{O_2} in our furnace assemblies is buffered at values approximating those of the Ni–NiO (N–NO) assemblage (Hill and Boettcher, unpublished data), runs made under N–NO conditions could be made with larger capsules, for an external solid buffer was not required. Thus, for runs under these conditions, approximately 35 mg of sample plus 19–26 wt percent H₂O were sealed in welded Ag₅₀Pd₅₀ tubing of 2.2 mm I.D. For runs made under Fe₃O₄–FeO (M–W) or Fe₃O₄–Fe₂O₃ (M–H) conditions, the double-capsule technique (Boettcher, Mysen, and Allen, 1973) originated by Eugster (1957) and used previously in piston-cylinder apparatus by Ganguly and Newton (1968), Lindsley and Munoz (1969), and Gilbert (1969) was employed. With this technique, only about 1.5 mg of sample plus 20–25 wt percent H₂O were sealed in Ag₅₀Pd₅₀ tubing of 1.5 mm I.D. These smaller capsules plus either the components for the M–W or the M–H buffer were in turn sealed in 3-mm O.D. Pt capsules. Possible water loss during preparation was determined by weighing the capsules before and after welding. Potential leaks in these capsules were detected by heating the capsules at 110°C for 12–24 hours and reweighing them. Optical and X-ray diffraction techniques were used to determine whether the M–W or M–H assemblages lasted the time of the experiments.

The samples were sealed in Ag₅₀Pd₅₀ rather than Pt in order to prevent loss of iron from the sample to the capsule (Merrill and Wyllie, 1973). Stern and Wyllie

TABLE 1a. Chemical Compositions of Rocks Used in the Experiments

	Andesite	Quartz tholeiite	Olivine tholeiite	Alkali basalt	Nephelinite
SiO ₂	59.10	50.71	49.71	46.01	38.57
TiO ₂	0.94	1.70	2.51	2.10	2.79
Al ₂ O ₃	17.8	14.48	12.74	13.89	11.71
Cr ₂ O ₃	—	—	—	0.065	0.06
Fe ₂ O ₃	1.78	4.89	3.23	4.29	5.21
FeO	4.83	9.07	8.40	8.96	7.78
MnO	0.10	0.22	0.17	0.19	0.11
MgO	3.05	4.68	10.31	10.01	13.08
CaO	6.85	8.83	10.73	10.36	12.84
SrO	—	—	—	0.05	—
BaO	—	—	—	0.03	0.08
Li ₂ O	—	—	—	< .01	—
Na ₂ O	4.27	3.16	1.97	2.59	4.22
K ₂ O	1.08	0.77	0.49	0.75	1.20
Rb ₂ O	—	—	—	0.00186	—
H ₂ O ⁺	0.1	1.04	0.07	0.17	0.59
H ₂ O [–]	—		0.00	0.00	0.19
P ₂ O ₅	0.22	0.36	0.27	0.33	1.11
CO ₂	—	—	—	0.05	0.27
F	—	—	—	0.04	—
	100.12	99.91	100.00	99.89	99.81
O = F				–0.02	
				99.87	
Mg/(Mg+Fe ²⁺)	0.53	0.48	0.69	0.66	0.75
Mg/(Mg+ΣFe)	0.46	0.38	0.62	0.58	0.65
Fe/Mg	1.17	1.62	0.62	0.72	0.54

(1975) report 30 and 40 wt percent iron loss from andesite–H₂O mixtures at 1100°C and 30 kbar in capsules of Ag₇₅Pd₂₅ and Ag₃₀Pd₇₀, respectively, but find that iron loss is not significant at 1000°C in runs of 10 hours. However, our data for runs with the andesite in 2.2-mm I.D. Ag₅₀Pd₅₀ capsules under N–NO conditions at temperatures below 1000°C suggest iron loss as high as 40 percent. Run number 50 (Table 2) contained approximately 80 percent glass with 1.01 percent total Fe (Table 7), 20 percent amphibole with 10.57 percent total Fe (Table 6), <1.0 percent orthopyroxene and a trace of an opaque mineral. These figures account for at least 58 percent of the 5.0 percent total Fe in the starting material (Table 1). Our runs with the andesite under M–W and M–H conditions were made with smaller capsules (1.5-mm I.D.) and afford a better comparison of our data with that of Stern and Wyllie. For example, run number 68 (Table 2) contains at least 85 percent glass with 1.32 percent total Fe (Table 7), at least 5 percent amphibole with 6.4 percent total Fe (Table 6), and <10 percent opaque mineral. These figures indicate no absorption of iron by the capsule. This is ex-

TABLE 1b. Normative Compositions (C.I.P.W.) of Rocks Used in the Experiments

	Andesite	Quartz tholeiite	Olivine tholeiite	Alkali basalt	Nephelinite
quartz	10.14	3.82	--	--	--
orthoclase	6.38	4.55	2.90	4.43	--
albite	36.13	26.74	16.67	21.54	--
anorthite	26.22	23.05	24.47	24.06	9.47
nepheline	--	--	--	0.20	19.34
leucite	--	--	--	--	5.56
diopside	5.21	15.18	21.67	20.28	26.16
wo	(2.65)	(7.69)	(11.28)	(10.52)	(13.80)
en	(1.43)	(3.99)	(7.71)	(7.00)	(10.56)
fs	(1.13)	(3.50)	(2.68)	(2.75)	(1.81)
hypersthene	11.07	14.39	23.99	--	--
en	(6.17)	(7.67)	(17.80)	--	--
fs	(4.90)	(6.72)	(6.19)	--	--
olivine	--	--	0.16	18.00	22.68
fo	--	--	(0.12)	(12.56)	(15.43)
fa	--	--	(0.04)	(5.44)	(2.91)
cs	--	--	--	--	(4.34)
magnetite	2.58	7.09	4.68	6.22	7.55
ilmenite	1.79	3.23	4.77	3.99	5.30
apatite	0.51	0.83	0.63	0.77	2.57

Mt. Hood andesite. See Wise (1969, p. 1002, #155).

Picture Gorge quartz tholeiite. Analyst: C.O. Ingamells, The Pennsylvania State University. (See also Hamilton et al., 1964, p. 23).

1921 Kilauea, Hawaii olivine tholeiite. Analyst: C.O. Ingamells, The Pennsylvania State University. (See also Fudali, 1965, p. 1065).

Prehistoric Hualalai, Hawaii alkali basalt. Analyst: J.B. Bodkin, The Pennsylvania State University. (See also Yoder and Tilley, 1962, p. 360).

Honolulu olivine nephelinite. See Winchell (1947, p. 30-31, analyses #15).

plicable in terms of the high f_{O_2} and low activity of metallic Fe (a_{Fe^0}) in the sample when using the M-H buffer.

Apparatus

All experiments were in piston cylinder apparatus similar to that described by Boyd and England (1960). Several runs made between 20 and 36 kbar used a 12.7-mm diameter furnace assembly and piston (Boettcher and Wyllie, 1968); in the remaining runs we used a 25.4-mm diameter furnace assembly and piston (Boettcher, in Johannes et al, 1971). Capsules were placed horizontally in the notched top surface of a cylinder of boron nitride that overlay a cylinder of talc and a disc of pyrophyllite. To avoid contamination of the thermocouple, a strip of Pt foil was placed between the capsule and the thermocouple, which passed successively through cylinders of Solenhofen limestone, pyrophyllite, and boron nitride in the upper part of the furnace assembly. These were surrounded by a cylindrical graphite furnace inside a cylinder of talc with a ring of fired pyrophyllite at the base of the talc cylinder. This furnace assembly was surrounded by a sheet of lead foil

TABLE 2. Run Data

Pres kbars	Temp °C	Run #	Starting material	Buffer	Wt% H ₂ O	Duration hrs.	Phase assemblage
10	920	140	andesite	N-NO	25.0	7.0	L, V, Am, qM, (Op), ?Opx
10	940	157	andesite	N-NO	25.0	7.0	L, V, Am, qM
10	960	199	andesite	N-NO	20.2	6.5	L, V, ?qM
13	900	50	andesite	N-NO	20.0	12.0	L, ?V, Am, Opx, Op
13	920	52	andesite	N-NO	20.0	12.5	L, V, Am, Opx, Op, qM
13	940	54	andesite	N-NO	19.9	12.5	L, ?V, Am, Opx, qM
13	960	56	andesite	N-NO	20.0	13.3	L, ?V
18	920	102	andesite	N-NO	20.0	11.3	L, ?V, Am, Opx, Ga, Op, qM, Ru
18	940	110	andesite	N-NO	22.6	12.5	L, V, Am, Ga, Op, qM
18	960	104	andesite	N-NO	25.0	12.0	L, V, qM
19	850	130	andesite	N-NO	25.0	22.0	L, V, Am, Ga, Opx, Ru
19	920	126	andesite	N-NO	25.0	23.0	L, V, Ga, (Op), qM
20	920	114	andesite	N-NO	24.9	22.3	L, ?V, Ga, Op, qM
20	960	425	andesite	N-NO	20.7	26.5	L, V, Ga, (Op), qM
20	975	230	andesite	N-NO	33.3	3.5	L, V, Ga, (Op), qM
20	980	423	andesite	N-NO	20.6	22.5	L, V, (Op), qM
23	1000	429	andesite	N-NO	21.0	22.5	L, V, Ga, (Op), qM
23	1020	424	andesite	N-NO	22.4	22.5	L, V, (Op), qM
10	940	202	andesite	M-W	21.1	4.5	L, V, Am, (Op)
10	960	209	andesite	M-W	20.2	4.5	L, V, Am, Op, qM
10	970	233	andesite	M-W	24.8	4.5	L, V, qM
13	900	94	andesite	M-W	20.0	4.5	L, ?V, Am, Opx, Op, Sp, Ru
13	940	88	andesite	M-W	20.0	4.5	L, ?V, Am, (Op)
13	960	93	andesite	M-W	20.0	4.5	L, V, qM
10	940	227	andesite	M-H	25.0	3.0	L, V, Am, Op, qM
10	960	222	andesite	M-H	25.0	3.0	L, V, Op
13	880	72	andesite	M-H	20.0	5.2	L, ?V, Am, Pl, Op
13	920	68	andesite	M-H	20.0	3.2	L, ?V, Am, Op
13	940	70	andesite	M-H	20.0	4.0	L, V, Am, Op, qM
13	960	223	andesite	M-H	25.0	4.3	L, V, Op, qM
10	920	179	qz thol	N-NO	21.0	15.5	L, V, Am, Cpx, Op, qM
10	940	194	qz thol	N-NO	20.0	5.0	L, V, Am, Cpx, Op, qM
10	960	173	qz thol	N-NO	20.1	6.5	L, V, Cpx, Op, qM
10	980	178	qz thol	N-NO	20.2	7.0	L, V, Cpx, qM
10	1000	142	qz thol	N-NO	25.0	7.0	L, V, qM
13	980	101	qz thol	N-NO	20.0	7.5	L, V, Am, Cpx, Op, qM
13	1000	45	qz thol	N-NO	19.0	14.3	L, V, Am, Cpx, qM
13	1020	53	qz thol	N-NO	18.2	12.0	L, V, qM
13	1040	42	qz thol	N-NO	19.0	12.0	L, V, qM, qAm
15	1000	170	qz thol	N-NO	20.0	7.0	L, V, Cpx, Am, Op, qM, qAm
18	960	108	qz thol	N-NO	23.4	14.3	L, V, Am, Cpx, Am, Op, qM, qAm
18	980	120	qz thol	N-NO	25.0	7.1	L, V, Cpx, Am, Op, qM:
18	1000	105	qz thol	N-NO	25.0	11.8	L, V, qM
20	960	112	qz thol	N-NO	24.8	22.7	L, V, Ga, Cpx, Op, qM
21	960	116	qz thol	N-NO	25.0	23.0	L, V, Ga, Cpx, Op, qM
10	960	215	qz thol	M-W	20.8	4.5	L, V, Am, Cpx, Op, qM, ?qAm
10	980	228	qz thol	M-W	20.0	4.5	L, V, Cpx, Op, qM
10	1000	197	qz thol	M-W	19.6	4.5	L, V, Cpx, qM, qAm
10	1020	289	qz thol	M-W	24.4	3.0	L, V, qM
13	940	400	qz thol	M-W	22.2	4.0	L, V, Cpx, Am, (Op), qM
13	960	396	qz thol	M-W	25.3	4.0	L, V, Cpx, Am, (Op), qM
13	980	89	qz thol	M-W	20.0	4.5	L, V, Cpx, Am, Op, qM
13	1000	86	qz thol	M-W	20.0	4.5	L, V, Cpx, Am, qM
13	1020	100	qz thol	M-W	20.0	4.5	L, V, (Op), qM
13	1060	98	qz thol	M-W	20.0	4.5	L, V, qM
10	940	226	qz thol	M-H	25.0	4.5	L, V, Cpx, Am, Op
10	960	235	qz thol	M-H	25.0	4.5	L, V, Cpx, Am, Op, qM, qAm
10	980	288	qz thol	M-H	25.4	3.0	L, V, Cpx, Op, qM, qAm
10	1000	224	qz thol	M-H	25.0	4.0	L, V, Cpx, Op, qM, qAm
10	1040	225	qz thol	M-H	25.0	4.5	L, ?V, Cpx, Op, qM
10	1060	234	qz thol	M-H	25.0	4.5	L, V, Op, qM
13	910	395	qz thol	M-H	25.3	4.0	L, V, Cpx, Am, Op, qM
13	920	76	qz thol	M-H	20.0	4.5	L, ?V, Cpx, Op, Am
13	940	78	qz thol	M-H	20.0	4.8	L, ?V, Cpx, Op, Am
13	960	71	qz thol	M-H	20.0	4.0	L, ?V, Cpx, Op
13	1000	57	qz thol	M-H	20.0	3.0	L, ?V, Cpx, Op, qM
13	1020	59	qz thol	M-H	20.0	6.0	L, V, Cpx, Op, qM
13	1040	67	qz thol	M-H	20.0	4.5	L, ?V, Cpx, Op
13	1060	84	qz thol	M-H	20.0	4.5	L, V, Op, qM, qCpx, qAm
13	1080	81	qz thol	M-H	20.0	4.5	L, ?V, Op, qCpx
10	1020	196	o1 thol	N-NO	20.3	5.5	L, V, Cpx, Am, qM, qAm
10	1040	198	o1 thol	N-NO	20.1	9.5	L, V, Cpx, qM, qAm
10	1060	181	o1 thol	N-NO	20.4	6.5	L, V, Cpx, qM
10	1080	193	o1 thol	N-NO	20.1	6.5	L, V, qM
13	1050	44	o1 thol	N-NO	19.0	12.0	L, V, Cpx, Am, qM
13	1070	47	o1 thol	N-NO	19.0	12.0	L, V, Cpx, qM
13	1085	51	o1 thol	N-NO	18.9	12.0	L, ?V, qM
16	1000	103	o1 thol	N-NO	20.0	11.8	L, V, Cpx, Am, Op, qM
16	1065	210	o1 thol	N-NO	20.5	7.0	L, V, Cpx, qM
18	1000	107	o1 thol	N-NO	24.1	12.0	L, V, Cpx, Am, Op, qM
20	1000	111	o1 thol	N-NO	25.0	12.4	L, V, Cpx, Am, Ga, Op, qM
20	1020	118	o1 thol	N-NO	25.1	22.5	L, V, Cpx, Am, Op, qM
20	1060	123	o1 thol	N-NO	25.0	7.0	L, V, Cpx, Am, qM
20	1080	131	o1 thol	N-NO	25.0	7.0	L, V, qM, qCpx
20	1097	128	o1 thol	N-NO	25.0	7.0	L, V, qM, qCpx, qAm
21	1000	115	o1 thol	N-NO	24.9	22.5	L, V, Cpx, Ga, Op, qM
10	960	205	o1 thol	M-W	20.6	4.5	L, V, Cpx, Am, Op, O1, qM
10	980	204	o1 thol	M-W	21.5	4.5	L, V, Cpx, Am, Op, O1, qM
10	1000	208	o1 thol	M-W	21.3	4.7	L, V, Cpx, Am, Op, O1, qM, qAm
10	1020	203	o1 thol	M-W	21.6	4.5	L, V, Cpx, (Op), qM
10	1060	229	o1 thol	M-W	20.0	4.8	L, V, Cpx, qM
10	1080	236	o1 thol	M-W	25.0	4.5	L, V, Op, qM

and lubricated with a slurry of MoS₂ and perfluorokerosene.

Temperatures were measured by Pt-Pt₉₀Rh₁₀ thermocouples, but they were not corrected for the effect of pressure on the emf. Friction corrections of -12 percent for the 12.7-mm furnace assemblies and -5 percent for the 25.4-mm furnace assemblies were ap-

TABLE 2, Continued

Pres kbars	Temp °C	Run #	Starting material	Buffer	Wt% H ₂ O	Dura- tion hrs.	Phase assemblage
13	980	401	ol thol	M-W	22.7	4.0	L, V, Cpx, Am, Ol, qM
13	1020	397	ol thol	M-W	25.0	4.2	L, V, Cpx, Am, qM
13	1040	96	ol thol	M-W	20.0	4.5	L, V, Cpx, Am, Ol, qM, qAm
13	1060	85	ol thol	M-W	20.0	4.5	L, V, Cpx, Am, qM
13	1080	146	ol thol	M-W	20.0	4.5	L, V, qM
13	1097	92	ol thol	M-W	20.0	4.7	L, V, qM
10	980	248	ol thol	M-H	25.0	3.2	L, V, Cpx, Am, Op, qM
10	1000	272	ol thol	M-H	25.4	3.3	L, V, Cpx, Op, qM
13	950	394	ol thol	M-H	20.2	4.0	L, V, Cpx, Am, Op, qM
13	980	77	ol thol	M-H	20.0	4.5	L, V, Cpx, Am, Op
13	1000	73	ol thol	M-H	20.0	4.9	L, V, Cpx, Op
13	1020	69	ol thol	M-H	20.0	4.8	L, V, Cpx, Op
13	1040	61	ol thol	M-H	20.0	5.0	L, V, Cpx, Op, qM
13	1060	82	ol thol	M-H	20.0	4.5	L, V, Cpx, Op, qM, qAm
13	1080	80	ol thol	M-H	20.0	4.5	L, V, Op, qM, qCpx, qAm
10	980	201	alk bas	N-NO	20.4	12.0	L, V, Ol, Cpx, Am, Op, qM
10	1000	174	alk bas	N-NO	20.2	6.5	L, V, Ol, Cpx, Am, qM, qAm
10	1020	186	alk bas	N-NO	20.3	22.0	L, V, Ol, Cpx, Am, qM, qAm
10	1040	172	alk bas	N-NO	20.0	6.5	L, V, Ol, Cpx, qM, qAm
10	1060	171	alk bas	N-NO	20.0	6.1	L, V, Ol, Cpx, qM, qAm
10	1080	139	alk bas	N-NO	25.0	7.1	L, V, Ol, Cpx, qM
10	1100	177	alk bas	N-NO	20.1	6.5	L, V, qM, qAm
13	1080	39	alk bas	N-NO	19.0	11.5	L, V, Ol, Cpx, Am, qM, qAm
13	1105	46	alk bas	N-NO	18.9	10.5	L, V, qM, qCpx
18	1040	109	alk bas	N-NO	24.5	13.1	L, V, Ol, Cpx, Am, qM
18	1097	106	alk bas	N-NO	25.0	10.7	L, V, qM, qCpx, qAm
20	1040	113	alk bas	N-NO	26.0	22.5	L, V, Ol, Cpx, Am, qM
20	1080	138	alk bas	N-NO	25.0	7.0	L, V, Ol, qM, qCpx, qAm
22	1040	117	alk bas	N-NO	25.0	22.3	L, V, Ol, Cpx, Am, qM
22	1060	121	alk bas	N-NO	25.0	23.0	L, V, Ol, Cpx, Am, qM
22	1097	125	alk bas	N-NO	25.0	7.0	L, V, qM, qAm, qCpx
24	1040	129	alk bas	N-NO	25.0	30.0	L, V, Ol, Cpx, Am, Ga, qM
26	1040	133	alk bas	N-NO	25.0	21.5	L, V, Ga, Cpx, Ol, qM, qAm
10	980	211	alk bas	M-W	21.9	4.7	L, V, Ol, Cpx, Am
10	1000	212	alk bas	M-W	21.5	4.5	L, V, Ol, Cpx, Am, qM, qAm
10	1020	213	alk bas	M-W	21.3	4.5	L, V, Ol, Cpx, qM, qAm
10	1040	218	alk bas	M-W	20.0	4.5	L, V, Ol, Cpx, qM, qAm
10	1080	290	alk bas	M-W	22.7	3.0	L, V, Ol, qM
13	1020	95	alk bas	M-W	19.7	4.5	L, V, Ol, Cpx, Am, qM, qAm
13	1040	91	alk bas	M-W	20.3	4.5	L, V, Ol, Cpx, Am, qM
13	1060	90	alk bas	M-W	20.0	4.5	L, V, Ol, qM, qAm, qCpx
13	1080	145	alk bas	M-W	20.0	4.5	L, V, Ol, qM, qAm, qCpx
13	1097	87	alk bas	M-W	20.0	4.8	L, V, ?Op, qM, qCpx
10	1000	270	alk bas	M-H	25.7	4.3	L, V, Cpx, Am, Op, qM
10	1020	271	alk bas	M-H	25.6	3.3	L, V, Cpx, Am, Op, qM
10	1040	257	alk bas	M-H	25.0	3.0	L, V, Cpx, Op, qM
13	1020	74	alk bas	M-H	20.0	4.5	L, V, Cpx, Am, Op
13	1040	75	alk bas	M-H	20.0	4.9	L, V, Cpx, Am, Op
13	1060	63	alk bas	M-H	20.0	4.0	L, V, Cpx, Op, qM, qAm
13	1097	83	alk bas	M-H	20.0	4.5	L, V, Op, qM, qAm, qCpx
13	1100	79	alk bas	M-H	20.0	5.3	L, V, Op, qAm, qCpx
10	1020	283	nephelinite	N-NO	19.9	5.0	L, V, Ol, Cpx, Am, qM
10	1040	286	nephelinite	N-NO	19.1	5.5	L, V, Ol, Cpx, (Am), qM
10	1060	292	nephelinite	N-NO	19.9	4.2	L, V, Ol, Cpx, qM
13	1020	265	nephelinite	N-NO	19.9	6.0	L, V, Ol, Cpx, Am, (Op), qM, qAm
13	1040	269	nephelinite	N-NO	19.9	4.2	L, V, Ol, Cpx, ?Am, qM, qAm
13	1060	261	nephelinite	N-NO	20.0	6.0	L, V, Ol, Cpx, qM
13	1080	275	nephelinite	N-NO	19.9	4.8	L, V, Ol, Cpx, qM
13	1100	263	nephelinite	N-NO	20.0	6.5	L, V, Ol, qM
13	1120	267	nephelinite	N-NO	20.0	4.0	L, V, qM
16	1040	278	nephelinite	N-NO	20.0	5.0	L, V, Ol, Cpx, qM
18	1120	291	nephelinite	N-NO	20.0	4.5	L, V, qM
19	1020	276	nephelinite	N-NO	20.3	7.0	L, V, Ol, Cpx, Am, Op, qM
20	1040	303	nephelinite	N-NO	20.1	6.2	L, V, Ol, Cpx, Am, Op, ?B ₁ , qM
20	1060	306	nephelinite	N-NO	20.1	6.3	L, V, Ol, Cpx, Am, Op, qM, qAm, qCpx
20	1100	282	nephelinite	N-NO	20.0	6.2	L, V, (Ol), qM, qCpx, qAm
22	1020	284	nephelinite	N-NO	20.1	21.0	L, V, Ol, Cpx, Am, Sp, Op, qM
22	1080	304	nephelinite	N-NO	20.0	6.0	L, V, Ol, Cpx, Op, qM, qAm
24	1060	300	nephelinite	N-NO	20.1	7.1	L, V, Ol, Cpx, Am, Op, ?B ₁ , qM
24	1080	308	nephelinite	N-NO	20.0	5.0	L, V, Ol, Cpx, Op, qM, qAm, qCpx
24	1105	305	nephelinite	N-NO	20.0	6.0	L, V, Ol, Cpx, Op, qM, qAm
24	1115	307	nephelinite	N-NO	20.0	6.0	L, V, (Ol), (?Op), qM, qAm, qCpx

TABLE 2, Continued

25	1020	285	nephelinite	N-NO	20.1	22.0	L, V, Ol, Cpx, Am, Op, qM
28	1020	310	nephelinite	N-NO	25.2	22.5	L, V, Ol, Cpx, Am, Op, qM
28	1040	326	nephelinite	N-NO	24.9	4.3	L, V, Ol, Cpx, Am, Op, qM, qAm
28	1060	319	nephelinite	N-NO	24.9	7.0	L, V, Ol, Cpx, Op, qM, qAm
28	1080	320	nephelinite	N-NO	25.1	4.0	L, V, Ol, Cpx, Op, qM, qAm
28	1125	309	nephelinite	N-NO	21.2	6.3	L, V, Cpx, Op, qM, qAm, qCpx
28	1155	316	nephelinite	N-NO	24.8	4.3	L, V, qM, qAm, qCpx
30	850	327	nephelinite	N-NO	25.5	23.1	L, V, Ol, Cpx, Ga, Am, Op, qM
30	900	313	nephelinite	N-NO	24.5	22.2	L, V, Ol, Cpx, Ga, Am, Op, qM
30	1020	287	nephelinite	N-NO	20.0	22.3	L, V, Ol, Cpx, Ga, Am, Op, qM
30	1100	323	nephelinite	N-NO	26.0	4.0	L, V, (?Ol), qM, qAm
31	1020	321	nephelinite	N-NO	26.4	23.0	L, V, Ol, Cpx, Ga, Am, Op, qM
32	900	328	nephelinite	N-NO	25.8	23.0	L, V, Ol, Cpx, Ga, Op, qM, qAm
32	1020	293	nephelinite	N-NO	24.4	24.0	L, V, Ol, Cpx, Ga, Op, qM
34	900	337	nephelinite	N-NO	25.4	25.3	L, V, Ol, Cpx, Ga, Op, qM, qAm
36	900	339	nephelinite	N-NO	25.3	20.0	L, V, Ol, Cpx, Ga, Op, qM, qAm
10	1020	336	nephelinite	M-W	23.0	6.0	L, V, Ol, Cpx, Am, (Op), qM
10	1040	340	nephelinite	M-W	22.3	7.5	L, V, Ol, Cpx, (Op), qAm, qM
13	1020	330	nephelinite	M-W	25.6	4.0	L, V, Ol, Cpx, Am, (Op), qM
13	1040	334	nephelinite	M-W	25.0	6.1	L, V, Ol, Cpx, (Op), qM, qAm
13	1060	332	nephelinite	M-W	25.1	4.1	L, V, Ol, Cpx, (Op), qM
10	1040	335	nephelinite	M-H	24.9	7.0	L, V, Cpx, Am, Op, qM
10	1060	338	nephelinite	M-H	25.1	7.0	L, V, Cpx, Op, qM, qAm
13	1020	329	nephelinite	M-H	25.5	4.0	L, V, Cpx, Am, Op, qM
13	1040	333	nephelinite	M-H	25.3	6.0	L, V, Cpx, Am, Op, qM
13	1060	331	nephelinite	M-H	25.1	4.0	L, V, Cpx, Op, qM, qAm

Abbreviations: *qt thol* = quartz tholeiite; *ol thol* = olivine tholeiite; *alk bas* = alkali basalt; *L* = glass interpreted to be quenched liquid; *V* = glass interpreted to be quenched vapor; *Am* = amphibole; *Cpx* = clinopyroxene; *Op* = orthopyroxene; *Ol* = olivine; *Op* = opaque mineral; *Ga* = garnet; *Bi* = Biotite; *Sp* = sphene; *Hu* = rutile; *M* = mica-calcic mineral; *Pl* = plagioclase; *q* = interpreted to have crystallized during the quench; *?* = questionable; *()* = trace amount.

plied; all runs used the piston-in method (Johannes *et al.*, 1971).

Run Procedure

A pressure of at least one kbar below that to be maintained during the run was first applied to the furnace assembly. Next, the temperature was increased to the appropriate value over a period of about ten minutes, and the pressure was then increased to the desired value. Synthesis runs lasted between three and 31 hours. To reverse the high-temperature part of the amphibole-out curves, two-stage runs were made. That is, a run under conditions known from previous runs to be sufficient to melt the entire charge was readjusted to within a few degrees less than the conditions known from previous synthesis runs to produce amphibole and held at those conditions from 21 to 40 hours. A similar procedure was used to reverse the high-pressure part of the same curves. In these, a run at a half kilobar above the pressure sufficient to form a garnet-bearing, amphibole-free assemblage was lowered to a half kilobar below the highest pressure at which amphibole was synthesized and held at these conditions from 22 to 40 hours.

Identification and Description of Phases

The phase assemblage at run conditions was determined by standard optical and X-ray diffraction

study of the quenched products. Mineral phases in amounts too small to be detected by X-ray diffraction techniques could usually be detected with the petrographic microscope, using the following characteristics.

Forsterite occurred as colorless, euhedral to subhedral, equidimensional crystals.

Clinopyroxene generally appeared as euhedral, colorless to faintly green prisms of moderate birefringence.

Orthopyroxene was characteristically in subhedral, medium-brown, squat prisms, showing faint pleochroism in some runs.

Amphibole occurred as slightly pleochroic, light-green to slightly yellow-green, tabular, subhedral to euhedral crystals with an extinction angle of 12° – 25° , often with twinning.

Plagioclase occurred as subhedral prisms with albite twins.

Garnet, although amber to rusty red under a low-power binocular microscope, formed colorless, isotropic euhedra.

Sphene occurred as brownish-red subhedral crystals, and rutile occurred as acicular dark reddish brown crystals of high birefringence.

Opaque oxides, although not identified further, occurred as subhedral to euhedral crystals.

Quenched silicate melt was a transparent, faintly lilac, isotropic glass.

Quenched vapor in most cases occurred as spheres ("fish roe"), sometimes arranged on fibers like beads, but was also as irregular masses. It was not easily distinguished from quenched liquid at pressures above 27 kilobars. Quench minerals include amphibole, clinopyroxene, and mica. The quench amphibole and quench clinopyroxene occurred as ragged skeletal crystals and ragged overgrowths on primary crystals. Quench micas occurred as colorless plates, often with ragged edges. A brown mica, which occurred in some runs with the alkali basalt and nephelinite at pressures of 20 kbar and above, may be primary.

Results

Phase Relationships

The results of experiments on the five starting materials are presented in Table 2. The phase relationships are shown in P - T projection in Figures 1-6. It was possible for us to predict the approximate configuration of the stability field of amphiboles in Figures 1-6 as a result of earlier work at high pressures by Lambert and Wyllie, 1968; Gilbert, 1969;

Hill and Boettcher, 1970; Essene, Hensen, and Green, 1970). This study accurately establishes these fields and shows the effects of varying bulk composition (from the olivine nephelinite with 38.57% SiO_2 to the andesite with 59.10% SiO_2) and f_{O_2} throughout the stability range of magnetite. The results of varying $f_{\text{H}_2\text{O}}$ will appear in a following paper. Although H_2O was the only volatile added to the starting materials, the mole fraction of H_2O in the vapor ($X_{\text{H}_2\text{O}}^{\text{v}}$) was slightly less than 1.0 because some solids dissolve in the vapor and also because $X_{\text{H}_2}^{\text{v}}$ ranges from 0.05 for M-W conditions to 0.01 for M-H conditions, assuming ideal mixing (Mysen and Boettcher, 1975a, b).

Amphibole in the Mt. Hood andesite, under approximately N-NO conditions (Fig. 1A), is stable on the vapor-saturated liquidus with or without spinel, to a temperature of about 950°C over a pressure range from at least as low as 10 kbar to as high as about 18 kbar. Our value of 950°C compares favorably with the work of Egger (1970) on the same andesite at 5.5 kbar. Under water-saturated conditions (9.7 wt% H_2O in the liquid), he reported a temperature of 955°C for the breakdown of amphibole. The amphibole-out curve acquires a rather small slope (dP/dT) at about 18 kbar where garnet becomes stable at the expense of amphibole. In the vicinity of the change in slope at about 18 kbar, the liquidus has a moderately steep positive slope (dP/dT) extending to our last datum point at 23 kbar and 1010°C ; garnet, with a minor amount of spinel, remains stable on the liquidus throughout this pressure range of about 5 kbar. Thus at temperatures of the amphibole-out curve, amphibole melts incongruently; and at pressures greater than those of the curve, amphibole-bearing assemblages transform to garnet-bearing assemblages. This general configuration is repeated in each of the other four rocks (Figs. 1B, 1C, 1D, and 3). In the andesite no detectable change occurred in the position of the liquidus or the stability of amphibole when using either the M-H or M-W buffers at 13 kbar, or the M-H buffer at 10 kbar; however, amphibole remained stable to a slightly higher temperature, 965°C , when using the M-W buffer at 10 kbar (Fig. 2A). It is of some interest to note that in two runs in which the capsule leaked and most of the water was lost, clinopyroxene instead of amphibole was the primary crystalline phase.

Amphibole and clinopyroxene, with or without spinel, coexist on the liquidus from about 13 kbar and 1010°C to 19 kbar and 980°C in the Picture Gorge quartz tholeiite under approximately N-NO

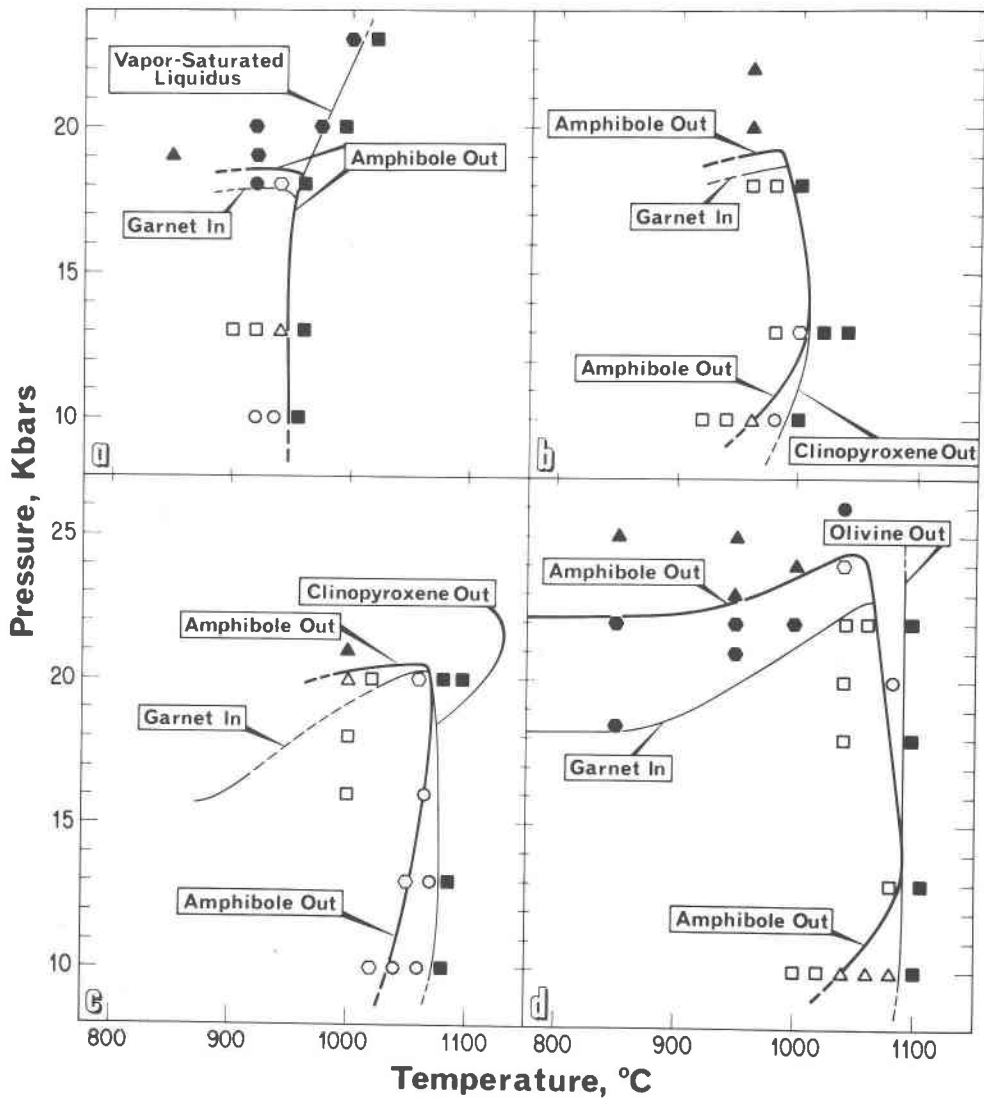


FIG. 1. Crystallization sequence for: (A) Mt. Hood andesite, (B) Picture Gorge quartz tholeiite, (C) 1921 Kilauea olivine tholeiite, (D) Hualalai alkali basalt. All assemblages coexist with liquid and vapor.

Legend:

(A) Andesite

- Am
- △ Am + Opx
- Am + Opx + Op
- Am + Op + Ga
- Am + Opx + Op + Ga
- ▲ Am + Opx + Ga
- Op + Ga
- Above liquidus

(B) Quartz Tholeiite

- Cpx
- △ Cpx + Op
- Am + Cpx + Op
- Am + Cpx
- ▲ Ga + Cpx + Op
- Above liquidus

(C) Tholeiite

- Cpx
- △ Am + Cpx + Ga + Op
- Am + Cpx + Op
- Am + Cpx
- ▲ Cpx + Ga + Op
- Above liquidus

(D) Alkali olivine basalt

- Ol
- △ Ol + Cpx
- Am + Ol + Cpx
- Am + Ol + Cpx + Ga
- Ol + Cpx + Ga
- ▲ Ol + Cpx + Ga + Ru + Op
- Am + Ol + Cpx + Ga + Ru + Op
- Above liquidus

conditions (Fig. 1B). At 10 kbar, clinopyroxene is the stable liquidus phase at a temperature of 990°C, and amphibole appears as an additional phase below 950°C. At pressures above 19 kbar, amphibole is un-

stable relative to the garnet-bearing assemblages. The slope of that part of the amphibole-out curve representing the upper-pressure stability probably extends to lower temperatures with a small dP/dT ,

based on the reversed brackets at 12 and 24 kbar and 700°C established by Essene *et al* (1970). The stability of amphibole at 10 kbar is increased 20° by employing either the M-W or M-H buffer (Fig. 2B); the stability of clinopyroxene (not shown) is increased 20° using the M-W buffer and by 60° using M-H. At 13 kbar, amphibole is stable on the liquidus to about 1010°C with M-W as with the N-NO buffer; however, under conditions of the M-H buffer, the stability is decreased 60° at 13 kbar, whereas the stability of clinopyroxene (not shown) is increased by 40°.

Melting relations for the 1921 Kilauea olivine tholeiite at approximately N-NO conditions are in

Figure 1C. Clinopyroxene is the sole crystalline liquidus phase up to 20 kbar, at which pressure it is joined by amphibole. At pressures above 20 kbar, a garnet-bearing assemblage replaces the amphibole-bearing assemblage. Hill and Boettcher (1970) determined the stability of amphibole at lower temperatures for this rock, but their value of 26 kbar at 700°C is too high because of the metastable persistence of amphibole in nonreversed runs. The stability of amphibole is increased by 10° at 13 kbar using M-W buffer (Fig. 2C), but increasing the f_{O_2} with M-H reduced the stability by 70°; however, the clinopyroxene liquidus remained at 1070°C for both buffers. Decreasing the pressure from 13 to 10 kbar

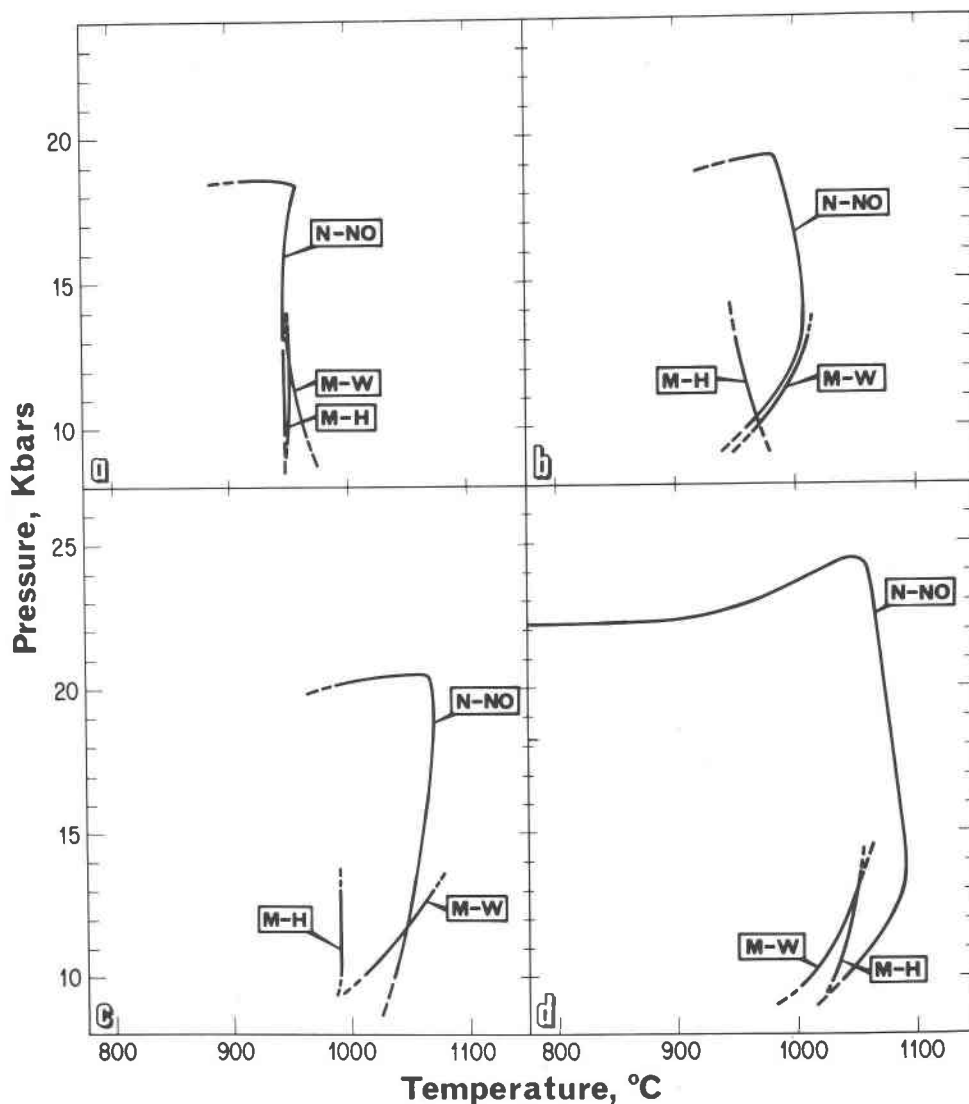


FIG. 2. Amphibole-out curves for (A) Mt. Hood andesite, (B) Picture Gorge quartz tholeiite, (C) 1921 Kilauea olivine tholeiite, and (D) Hualalai alkali basalt under M-W, N-NO, and M-H conditions.

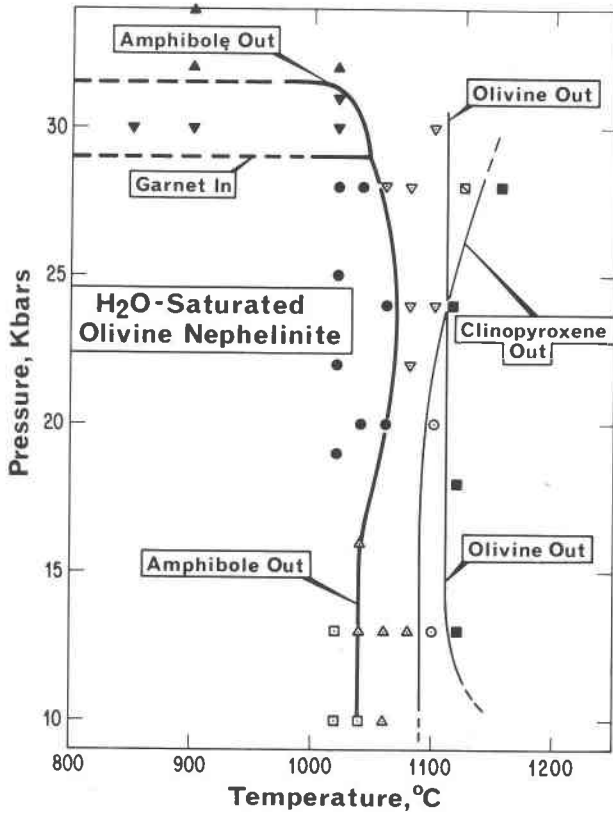


FIG. 3. Crystallization sequence for Honolulu olivine nephelinite. All assemblages coexist with liquid and vapor. Legend for Fig. 3 (for abbreviations, see Table 2):

- Ol, Cpx, Am ■ Above liquidus ▨ Cpx, Op
- △ Ol, Cpx ● Ol, Cpx, Am, Op ▾ Ol, Cpx, Am, Ga, Op
- Ol ▿ Ol, Cpx, Op ▲ Ol, Cpx, Ga, Op

caused the stability of amphibole to decrease by 30°C for the N-NO buffer, by 60°C for the M-W buffer, but to remain unchanged under M-H conditions (Fig. 2C).

The most refractory amphiboles in this study are those in the prehistoric Hualalai alkali olivine basalt (Fig. 1D). Olivine is the liquidus phase at all pressures from 10 to 26 kbar at approximately N-NO conditions. Amphibole was stable to the highest temperature, 1090°C, at 13 kbar and approximately N-NO conditions. The upper pressure stability limit is about 25 kbar, at which pressure an amphibole-bearing assemblage is replaced by a garnet-bearing assemblage, and the amphibole-out curve proceeds to lower temperatures with a small positive dP/dT . Our results for this curve are in agreement with those established at 700° to 900°C on a similar rock by Essene *et al* (1970). At 13 kbar, lowering f_{O_2} with the M-W buffer or raising f_{O_2} with M-H reduce the

maximum stability of amphibole by 40°C (Fig. 2D). Olivine is also the liquidus phase with the M-W buffer, but no olivine was found under M-H conditions; instead clinopyroxene was the liquidus phase.

Melting relations in the olivine nephelinite at approximately N-NO conditions are shown in Figure 3. Olivine is the sole crystalline liquidus phase from 10 to 24 kbar, above which it is replaced by clinopyroxene. The amphibole-out curve has a temperature maximum of 1070°C at 22 to 24 kbar, but decreases to 1050° at 28 kbar and 1040° at 10 to 13 kbar. The pressure maximum for this curve occurs at 31.5 kbar and 1030°C. This represents the highest pressure for any *reversed* amphibole-out curve yet reported. Lowering the f_{O_2} with the M-W buffer decreased the stability of amphibole by 10° at 10 and 13 kbar (Table 2); increasing f_{O_2} with the M-H increased the

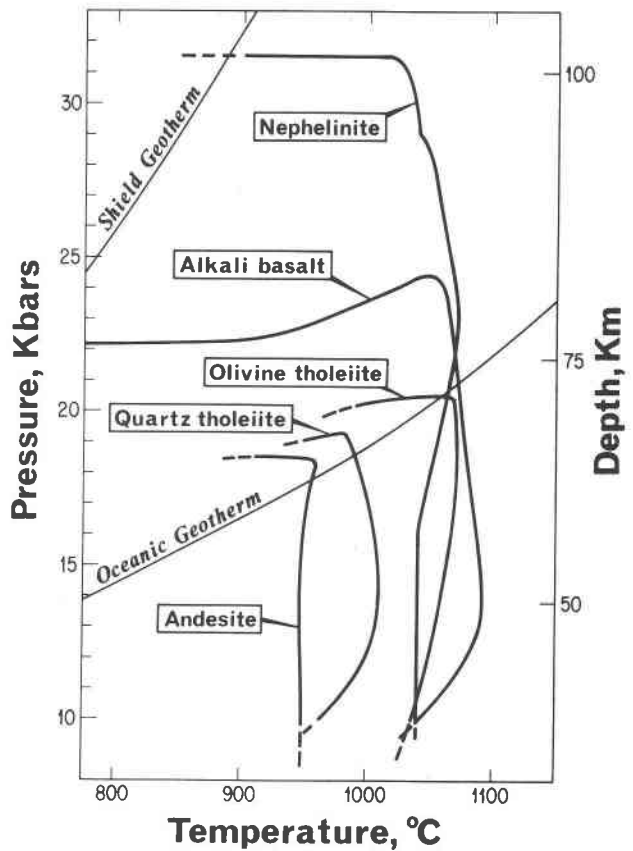


FIG. 4. Pressure-temperature projection showing the relative positions of the amphibole-out curves under N-NO conditions for the Mt. Hood andesite, Picture Gorge quartz tholeiite, 1921 Kilauea olivine tholeiite, Hualalai alkali basalt, and Honolulu olivine nephelinite along with the shield geotherm from Clark and Ringwood (1964) and oceanic geotherm from Ringwood, MacGregor, and Boyd (1964).

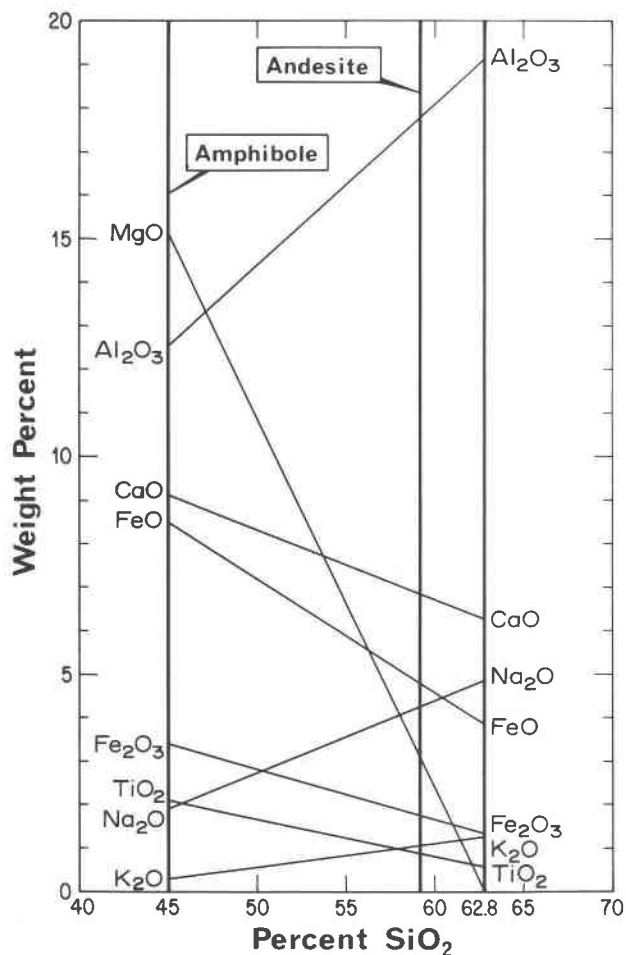


FIG. 5. Subtraction diagram. Mt. Hood andesite minus approximately 20 percent amphibole yields composition in right column.

stability 10°. Olivine was a stable crystalline phase with only the N-NO and M-W buffers. Our results on the stability of the pargasitic amphiboles (Table 6) synthesized in the alkali basalt and the nephelinite are consistent with the work of Boyd (1959) and Holloway (1973) on pargasite at pressures from 250 bars to 8 kbar.

We performed a brief investigation of the stability of amphibole in a basanite (Winchell, 1947, p. 30-31, analysis no. 13 with 42.86% SiO₂ and 10.51% normative nephelinite) at approximately N-NO conditions. Here, amphibole (with olivine and clinopyroxene) is stable to 1080°C at pressures of 13 to 16 kbar, although it is not present on the liquidus.

Chemical Analyses

The chemical compositions of olivines, pyroxenes, amphiboles, garnets, and glasses were determined

with an ARL-AMX electron microprobe analyzer (Tables 3-7). Although results are shown up to as many as four significant figures, they almost certainly are accurate only to two or three. Salient features of these determinations are as follows:

Olivine. Olivine occurs in significant amounts in only two of the rocks, the alkali basalt and the nephelinite, although there were trace amounts in the olivine tholeiite. The four analyses of these olivines in Table 3 indicate that the Mg/(Mg+ΣFe) of the olivine increases with that of the starting material.

Garnet. Garnet occurs at high pressures in all five rocks. The chemistry of these garnets (Table 4) indicates that the Mg/(Mg+ΣFe) is proportional to that of the starting material and that the pyrope content increases with pressure.

Clinopyroxene. Near liquidus temperatures, clinopyroxene is the most abundant mineral in the three basalts and in the nephelinite, but is undetected in the andesite. Mg/(Mg+ΣFe) of the clinopyroxene increases with that of the starting material (Table 5), but it decreases with increasing pressure in the quartz tholeiite and the olivine tholeiite and appears to be independent of pressure in the nephelinite. Clinopyroxenes synthesized under approximately N-NO conditions show larger values of Al₂O₃ and Na₂O compared to those at higher or lower values of *f*_{O₂}.

Amphibole. Although present in only minor

TABLE 3. Olivine Compositions

Analysis Rock	1 Alkali basalt	2 Alkali basalt	3 Alkali basalt	4 ^x Nephelinite
T°C	1020	1040	1040	1060
P, Kbar	13	18	24	24
Buffer	M-W	N-NO	N-NO	N-NO
SiO ₂	39.38	39.31	39.14	39.1
Al ₂ O ₃	0.25	0.23	0.34	0.04
FeO*	21.51	24.58	23.64	18.2
MgO	40.03	36.68	36.54	40.8
CaO	n.d.	0.40	0.21	0.4
TOTAL	101.17	101.20	99.87	98.54
Cations/4 Oxygens				
Si	1.004	1.017	1.012	1.006
Al	0.008	0.007	0.011	0.001
Fe	0.459	0.532	0.537	0.392
Mg	1.522	1.414	1.479	1.566
Ca	n.d.	0.011	0.006	0.011
ΣX	1.981	1.946	2.016	1.958
Mg/(Mg+Fe)	0.77	0.73	0.73	0.80

*Total, iron as FeO.

^xB.O. Mysen, Analyst.

TABLE 4. Garnet Compositions

Analysis	1	2	3	4	5
Rock	Andesite	Andesite	Quartz tholeiite	Quartz tholeiite	Alkali basalt
T°C	920	920	960	960	1040
P, Kbar	18	20	20	21	26
Buffer	N-NO	N-NO	N-NO	N-NO	N-NO
SiO ₂	41.59	45.40	38.41	39.19	40.41
TiO ₂	1.68	1.55	1.24	1.64	0.64
Al ₂ O ₃	19.88	17.51	19.41	18.95	21.20
FeO*	19.18	19.00	23.32	22.16	15.86
MgO	8.06	8.48	6.53	9.04	13.82
CaO	9.44	9.43	10.55	8.13	8.00
TOTAL	99.83	101.37	99.47	99.10	99.94
	Cations/24 Oxygens				
Si	6.277	6.696	6.003	6.136	6.535
Al	3.537	3.044	3.577	3.502	4.011
Ti	0.191	0.171	0.146	0.193	0.077
Fe	2.421	2.343	3.049	2.906	2.129
Mg	1.812	1.865	1.520	2.113	3.307
Ca	1.527	1.491	1.768	1.365	1.376
Mg/(Mg+ΣFe)	0.43	0.44	0.33	0.42	0.61

*Total iron as FeO.

amounts near the high-temperature part of the amphibole-out curve, amphibole rapidly increases in amount at lower temperatures. In computing the chemical analyses, the raw counts were corrected by the method of Bence and Albee (1968) with an APL program prepared by V. J. Wall. This program uses an estimated Fe₂O₃/FeO and H₂O content. H₂O was arbitrarily taken as 2.00 percent; Fe₂O₃/FeO values of 0.3, 0.4, and 0.8 were selected for M-W, N-NO, and M-H buffers, respectively. These values are not inconsistent with the range of values listed in the amphibole analyses in Leake (1968).

In view of the diversity in chemistry of the starting materials and the range of pressure, temperature, and *f*_{O₂} covered in this investigation, the amphiboles are remarkably similar in composition (Table 6). According to the classification devised by Leake (1968), they straddle the calciferous-subcalciferous boundary, and all of them fall in the pargasite-tschermakite-tschermakitic hornblende category. Only seven contain enough titanium to justify the prefix titaniferous (>0.25 Ti per 24 oxygens). Except for the amphiboles from the olivine tholeiite (possibly due to an error in the analysis of MgO and FeO in analysis 21, Table 6), Mg/(Mg+ΣFe) increases with that of the starting material. The amphiboles in the andesite become less magnesian with increasing pressure at conditions approximately N-NO, similar to the trend found by Mysen and Boettcher (1975b) for

amphibole in peridotites at high pressures. However, the amphiboles in the quartz tholeiite, the alkali basalt, and the nephelinite maintain a rather constant Mg/(Mg+ΣFe), which is lower than that of the clinopyroxenes.

Glasses. Two representative chemical analyses of glasses (quenched liquids) from the andesite are listed in Table 7. These glasses are highly aluminous and quartz-normative. They contain less Na₂O and more K₂O than their associated amphiboles.

Discussion

As suggested by Lambert and Wyllie (1968), the stability of amphiboles in andesites and basalts is limited by melting reactions at high temperatures and by transformation to garnet-bearing assemblages at high pressures. Amphiboles are stable to higher pressures and, with the exception of the nephelinite, to higher temperatures in order of decreasing activity of silica of the starting materials (Fig. 5). Although Mysen and Boettcher (1975a) found that the stability of amphibole in peridotites increases with increasing Mg/(Mg+Fe²⁺) of the starting material, this is not true for these five rocks. The ratios Mg/(Mg+Fe²⁺+Ca) and Mg/(Mg+ΣFe+Ca) of the starting materials were also examined in this regard, but no obvious relationships were found. All minerals in the five rocks, for which we have comparative analyses, show a strong positive correlation between the Mg/(Mg+ΣFe) of the mineral and that of the parent starting material.

No orthopyroxene was found in any of the three basalts, nephelinite, or the basanite under any of the conditions investigated by us. Green (1970, 1971, 1973) and Bultitude and Green (1968, 1971), have proposed a major role for orthopyroxene in the derivation of SiO₂-poor magmas, such as olivine nephelinites, from a hydrous pyrolite mantle. They report a small stability field of orthopyroxene in basanites and olivine nephelinites in the presence of 2 to 7 percent water. It is difficult to compare our results with theirs, for their runs were not under water-saturated conditions and were at different (uncontrolled) conditions of *f*_{O₂}; however, the lack of orthopyroxene in our basaltic rocks certainly restricts the potential *P-T-X* conditions under which fractional crystallization of orthopyroxene is an important mechanism. We are now investigating the stability of amphiboles in the andesite and the olivine tholeiite under vapor-saturated conditions in which *X*_{H₂O}^Y is varied by dilution with CO₂. No orthopyroxene has been found in runs made with the

TABLE 5. Clinopyroxene Compositions

Analysis	1	2	3	4	5	6	7	8	9	10
Rock	Quartz tholeiite						Olivine tholeiite			
T, °C	920	980	980	960	960	960	960	980	1050	1000
P, Kbar	13	13	13	18	20	21	10	13	13	18
Buffer	M-H	M-W	N-NO	N-NO	N-NO	N-NO	M-W	M-H	N-NO	N-NO
SiO ₂	51.46	52.25	51.87	48.03	48.99	49.74	50.56	50.58	51.47	52.95
TiO ₂	0.39	0.53	0.49	0.35	0.68	0.57	0.79	0.77	0.87	0.75
Al ₂ O ₃	6.20	2.80	2.17	4.62	4.39	5.83	2.76	2.54	2.75	2.57
FeO*	9.06	11.36	9.37	10.23	12.50	9.04	5.84	6.35	5.51	6.68
MgO	11.72	12.35	14.86	13.69	13.01	11.73	17.43	17.76	15.37	16.51
CaO	19.57	19.90	20.66	19.91	18.83	21.84	19.95	19.59	20.27	20.71
Na ₂ O	0.87	0.29	0.29	0.60	0.76	0.74	0.28	0.27	0.24	0.26
TOTAL	99.27	99.48	99.70	97.44	99.15	99.48	97.61	97.87	96.48	100.44
Cations/6 Oxygens										
Si	1.914	1.963	1.937	1.883	1.899	1.868	1.900	1.900	1.960	1.935
Al	0.272	0.124	0.096	0.216	0.201	0.258	0.122	0.117	0.127	0.111
Ti	0.011	0.015	0.014	0.011	0.020	0.016	0.022	0.023	0.025	0.021
Fe	0.282	0.357	0.293	0.339	0.407	0.284	0.184	0.207	0.180	0.204
Mg	0.649	0.691	0.827	0.808	0.755	0.656	0.976	1.032	0.894	0.899
Ca	0.780	0.801	0.827	0.837	0.793	0.879	0.803	0.819	0.827	0.811
Na	0.063	0.021	0.021	0.046	0.058	0.054	0.021	0.021	0.019	0.019
$\frac{Mg}{(Mg+\Sigma Fe)}$	0.70	0.66	0.74	0.70	0.65	0.70	0.84	0.83	0.83	0.82
Mg	37.9	37.4	42.5	40.7	38.6	36.1	49.7	50.1	47.0	47.0
Fe	16.5	19.3	15.0	17.1	20.8	15.6	9.4	10.1	9.5	10.7
Ca	45.6	43.3	42.5	42.2	40.6	48.3	40.9	39.8	43.5	42.3
Analysis	11	12	13	14	15	16	17	18	19	20
Rock	Ol. Thol.	Alkali basalt						Nephelinite		
T, °C	1000	1020	1040	1040	1040	1040	1040	1015	1015	1060
P, Kbar	21	13	13	18	20	24	26	19	19	24
Buffer	N-NO	M-W	M-H	N-NO	N-NO	N-NO	N-NO	N-NO	N-NO	N-NO
SiO ₂	49.64	49.67	49.31	51.33	51.71	48.90	51.11	50.55	49.94	52.8
TiO ₂	0.74	1.39	1.21	0.55	0.45	0.69	0.85	n.d.	n.d.	0.8
Al ₂ O ₃	5.14	3.94	6.64	3.60	2.11	4.66	5.47	3.25	3.42	3.6
FeO*	8.30	8.47	8.67	6.33	5.88	5.69	8.77	5.11	4.93	4.6
MgO	15.23	13.69	16.23	16.71	15.70	15.93	13.91	16.41	16.03	14.8
CaO	20.76	21.54	18.91	21.12	23.72	20.75	20.03	23.44	23.98	22.1
Na ₂ O	0.46	0.45	0.45	0.29	0.35	0.43	0.83	0.43	0.36	0.4
TOTAL	100.26	99.15	101.40	99.93	99.93	97.05	100.97	99.19	98.66	99.1
Cations/6 Oxygens										
Si	1.841	1.872	1.801	1.890	1.916	1.867	1.876	1.883	1.873	1.952
Al	0.225	0.175	0.286	0.156	0.092	0.210	0.237	0.143	0.151	0.153
Ti	0.021	0.039	0.033	0.015	0.013	0.020	0.024	--	--	0.022
Fe	0.258	0.267	0.265	0.195	0.182	0.187	0.269	0.159	0.155	0.140
Mg	0.842	0.769	0.883	0.917	0.867	0.934	0.761	0.911	0.896	0.800
Ca	0.825	0.870	0.740	0.833	0.942	0.849	0.788	0.935	0.964	0.859
Na	0.033	0.033	0.032	0.021	0.025	0.033	0.059	0.031	0.026	0.026
$\frac{Mg}{(Mg+\Sigma Fe)}$	0.77	0.74	0.77	0.82	0.83	0.83	0.74	0.85	0.85	0.85
Mg	43.7	40.3	46.8	47.1	43.5	47.4	41.9	45.4	44.5	44.5
Fe	13.4	14.0	14.0	10.0	9.1	9.5	14.8	7.9	7.7	7.8
Ca	42.9	45.7	39.2	42.8	47.3	43.1	43.3	46.7	47.8	47.7

*Analyst, B. O. Mysen.

*Total Iron as FeO.

TABLE 6a. Amphibole Compositions

Analysis	1	2	3	4	5	6	7	8	9	10 ^x	11	12	13	
Rock	Andesite										Quartz tholeiite			
T, °C	920	920	900	900	920	940	880	880	900	920	920	920	960	
P, Kbar	10	10	13	13	18	10	13	13	13	13	10	10	10	
Buffer	N-NO	N-NO	N-NO	N-NO	N-NO	M-W	M-H	M-H	M-W	M-H	N-NO	N-NO	M-W	
SiO ₂	45.54	45.00	46.68	45.56	43.81	44.63	47.07	46.59	44.59	43.2	42.01	41.54	42.61	
TiO ₂	2.01	2.10	1.36	1.33	1.21	2.30	0.39	0.44	1.25	0.63	2.19	1.93	2.75	
Al ₂ O ₃	12.50	12.55	11.71	11.34	14.69	11.66	14.04	13.59	12.81	14.6	12.69	12.87	12.36	
Fe ₂ O ₃ *	3.70	3.40	3.83	4.00	4.12	2.42	6.99	7.87	3.06	3.82	4.55	4.78	3.47	
FeO	9.24	8.50	9.58	10.01	10.30	8.06	8.74	9.83	10.20	4.78	11.38	11.96	11.57	
MgO	14.13	15.14	13.42	13.95	11.68	14.75	10.47	10.01	14.14	14.06	11.77	12.74	13.35	
CaO	8.18	9.16	9.05	10.26	9.34	10.84	7.80	8.49	9.49	9.8	9.00	9.92	10.02	
Na ₂ O	2.17	1.92	2.38	2.22	2.52	2.04	2.34	2.24	1.79	3.3	2.48	2.40	2.00	
K ₂ O	0.35	0.34	0.33	0.32	0.55	0.33	0.24	0.23	0.51	0.46	0.51	0.47	0.73	
H ₂ O*	2.00	2.00	2.00	2.00	2.00	2.00	2.00	2.00	2.00	--	2.00	2.00	2.00	
TOTAL	99.82	100.11	100.34	100.99	100.22	99.03	100.08	101.29	99.84	94.65	98.58	100.61	100.86	
$\frac{Mg}{Mg+Fe}$	0.67	0.70	0.65	0.65	0.60	0.72	0.55	0.51	0.66	0.75	0.58	0.58	0.62	
$\frac{Mg}{Mg+Fe^{2+}}$	0.73	0.76	0.71	0.71	0.67	0.77	0.68	0.64	0.71	0.84	0.65	0.66	0.67	
Analysis	14	15	16	17	18	19	20	21	22	23	24	25	26	27
Rock	Quartz tholeiite			Olivine tholeiite							Alkali basalt			
T, °C	910	910	950	950	950	980	980	1000	1000	980	980	980	980	1040
P, Kbar	13	13	13	13	13	13	13	18	20	10	10	10	10	13
Buffer	M-H	M-H	M-H	M-H	M-H	M-W	M-W	N-NO	N-NO	M-W	N-NO	N-NO	N-NO	M-H
SiO ₂	43.19	43.77	42.55	43.02	43.95	46.12	45.47	42.39	40.05	45.12	43.58	43.37	41.72	41.61
TiO ₂	2.10	1.87	1.45	1.40	1.25	3.76	4.28	2.42	1.38	2.59	2.88	2.88	2.35	1.52
Al ₂ O ₃	15.15	15.65	13.88	13.95	13.25	13.91	13.54	17.09	15.42	15.76	13.06	13.04	13.28	13.42
Fe ₂ O ₃ *	6.08	5.43	3.36	4.11	3.60	2.58	2.91	5.17	2.17	1.96	2.99	3.15	2.97	7.32
FeO	7.61	6.78	4.20	5.13	4.49	8.58	9.71	12.92	5.41	6.54	7.47	7.87	7.42	9.15
MgO	12.11	13.52	16.58	16.44	16.64	10.26	9.42	10.06	14.76	12.70	14.13	14.43	14.76	13.59
CaO	10.11	9.25	12.65	11.76	11.59	10.56	11.47	8.79	17.14	9.55	10.07	11.89	10.76	9.86
Na ₂ O	2.10	1.87	2.05	2.34	1.59	1.35	1.53	0.12	0.61	1.75	2.35	2.12	2.34	2.50
K ₂ O	0.56	0.60	0.53	0.53	0.55	0.58	0.55	0.37	0.01	0.73	0.72	0.72	0.78	0.74
H ₂ O*	2.00	2.00	2.00	2.00	2.00	2.00	2.00	2.00	2.00	2.00	2.00	2.00	2.00	2.00
TOTAL	101.01	100.74	99.25	100.68	98.91	99.70	100.88	101.33	98.95	98.70	99.25	100.47	98.38	101.71
$\frac{Mg}{Mg+Fe}$	0.62	0.67	0.80	0.77	0.79	0.63	0.58	0.51	0.78	0.73	0.71	0.71	0.72	0.61
$\frac{Mg}{Mg+Fe^{2+}}$	0.74	0.78	0.88	0.85	0.87	0.68	0.63	0.58	0.83	0.78	0.77	0.77	0.78	0.73
Analysis	28 ^x	29	30	31	32	33 ^x	34 ^x	35 ^x	36 ^x	37 ^x				
Rock	Nephelinite													
T, °C	1020	1015	1015	1015	1015	1015	1060	1020	1020	1020				
P, Kbar	13	19	19	19	19	19	24	28	13	13				
Buffer	N-NO	N-NO	N-NO	N-NO	N-NO	N-NO	N-NO	N-NO	M-W	M-H				
SiO ₂	42.0	42.60	42.01	43.14	42.49	44.51	42.38	42.20	39.3	41.6				
TiO ₂	1.62	1.73	1.66	1.70	1.62	1.65	2.10	0.78	2.18	1.18				
Al ₂ O ₃	13.4	15.81	15.43	13.44	13.42	14.23	13.8	15.3	13.8	13.32				
Fe ₂ O ₃ *	2.23	2.10	2.06	2.12	2.14	2.10	1.94	2.56	2.12	3.40				
FeO	5.57	5.25	5.16	5.29	5.34	5.26	4.86	6.4	7.08	7.25				
MgO	16.3	16.06	15.14	16.45	16.96	16.83	16.6	14.9	15.0	17.6				
CaO	11.4	10.71	11.78	11.68	11.72	10.85	11.3	10.93	11.38	10.84				
Na ₂ O	2.7	2.07	2.29	2.33	2.46	2.15	2.6	2.84	3.4	3.52				
K ₂ O	1.22	1.48	1.38	1.35	1.20	1.51	0.84	1.35	0.95	0.91				
H ₂ O*	--	2.00	2.00	2.00	2.00	--	--	--	--	--				
TOTAL	96.44	99.81	98.91	99.50	99.35	99.09	96.42	97.26	95.21	99.62				
$\frac{Mg}{Mg+Fe}$	0.79	0.80	0.79	0.80	0.81	0.81	0.82	0.75	0.75	0.75				
$\frac{Mg}{Mg+Fe^{2+}}$	0.84	0.84	0.84	0.85	0.85	0.85	0.86	0.81	0.79	0.81				

*Estimate, See Text.

xAnalyst, B. O. Myesen.

xAnalyst, B. O. Myesen

TABLE 6b. Chemical Formulae (O-23) for Amphiboles in Table 6a

Formula	1	2	3	4	5	6	7	8	9	10	11	12	13	14	15	16	17	18	19
Si	6.536	6.438	6.683	6.541	6.342	6.472	6.719	6.643	6.450	6.352	6.261	6.110	6.209	6.177	6.211	6.127	6.129	6.312	6.594
Al ^{IV}	1.464	1.562	1.317	1.459	1.658	1.528	1.281	1.357	1.550	1.648	1.739	1.890	1.791	1.823	1.789	1.873	1.871	1.688	1.406
Al ^{VI}	0.652	0.556	0.660	0.461	0.850	0.467	1.083	0.929	0.636	0.884	0.492	0.343	0.333	0.733	0.830	0.485	0.473	0.557	0.940
Ti	0.217	0.226	0.146	0.144	0.132	0.251	0.042	0.047	0.136	0.070	0.245	0.213	0.301	0.226	0.200	0.157	0.150	0.135	0.404
Fe ³⁺	0.400	0.366	0.413	0.432	0.449	0.264	0.751	0.845	0.333	0.423	0.511	0.529	0.381	0.655	0.580	0.364	0.441	0.389	0.278
Mg	3.022	3.228	2.863	2.985	2.520	3.188	2.227	2.127	3.048	3.081	2.614	2.793	2.899	2.581	2.859	3.558	3.490	3.562	2.186
Fe ²⁺	1.109	1.017	1.147	1.202	1.247	0.978	1.043	1.172	1.234	0.588	1.419	1.471	1.410	0.910	0.805	0.506	0.611	0.539	1.026
Ca	1.258	1.404	1.388	1.578	1.449	1.684	1.193	1.297	1.471	1.544	1.437	1.563	1.565	1.549	1.406	1.952	1.795	1.784	1.618
Na	0.604	0.533	0.661	0.618	0.707	0.574	0.648	0.619	0.502	0.941	0.717	0.684	0.565	0.582	0.515	0.572	0.646	0.443	0.374
K	0.064	0.062	0.060	0.059	0.102	0.061	0.044	0.042	0.094	0.086	0.097	0.088	0.136	0.102	0.109	0.097	0.096	0.101	0.106
Ca+Na+K	1.926	1.999	2.109	2.255	2.258	2.319	1.885	1.958	2.067	2.571	2.251	2.335	2.266	2.233	2.030	2.621	2.537	2.328	2.098
mg	0.67	0.70	0.65	0.65	0.60	0.72	0.55	0.51	0.66	0.75	0.58	0.58	0.62	0.62	0.67	0.80	0.77	0.79	0.63
Classification*	t.h.	t.	t.h.	t.h.	t.	t.	t.h.	t.h.	t.	p.	t.	t.	t.h.						
Fe/Mg	0.50	0.43	0.54	0.55	0.67	0.40	0.81	0.95	0.51	0.33	0.74	0.72	0.62	0.61	0.48	0.24	0.30	0.26	0.60

Formula	20	21	22	23	24	25	26	27	28	29	30	31	32	33	34	35	36	37
Si	6.500	6.092	5.853	6.445	6.312	6.195	6.139	6.024	6.145	6.090	6.087	6.218	6.146	6.273	6.151	6.127	5.906	5.970
Al ^{IV}	1.500	1.908	2.147	1.555	1.688	1.805	1.861	1.976	1.855	1.910	1.913	1.782	1.854	1.727	1.849	1.873	2.094	2.030
Al ^{VI}	0.783	0.989	0.511	1.100	0.543	0.392	0.444	0.316	0.457	0.756	0.724	0.503	0.436	0.639	0.513	0.747	0.352	0.225
Ti	0.460	0.262	0.152	0.278	0.314	0.309	0.260	0.166	0.178	0.186	0.181	0.184	0.176	0.175	0.229	0.085	0.246	0.127
Fe ³⁺	0.313	0.559	0.239	0.211	0.326	0.339	0.329	0.798	0.246	0.226	0.225	0.230	0.233	0.223	0.212	0.280	0.240	0.367
Mg	2.007	2.155	3.215	2.704	3.050	3.072	3.237	2.932	3.554	3.422	3.270	3.534	3.656	3.535	3.590	3.224	3.360	3.764
Fe ²⁺	1.161	1.553	0.661	0.781	0.905	0.940	0.913	1.108	0.682	0.628	0.625	0.638	0.646	0.620	0.590	0.777	0.890	0.870
Ca	1.757	1.354	2.684	1.462	1.563	1.820	1.697	1.530	1.787	1.641	1.829	1.804	1.816	1.639	1.757	1.701	1.833	1.667
Na	0.424	0.033	0.173	0.485	0.660	0.587	0.668	0.702	0.766	0.574	0.643	0.651	0.690	0.588	0.732	0.800	0.991	0.979
K	0.100	0.068	0.002	0.133	0.133	0.131	0.146	0.137	0.228	0.270	0.255	0.248	0.221	0.272	0.156	0.250	0.182	0.167
Ca+Na+K	2.281	1.455	2.859	2.080	2.356	2.538	2.511	2.369	2.781	2.485	2.727	2.703	2.727	2.499	2.645	2.751	3.006	2.813
mg	0.58	0.51	0.78	0.73	0.71	0.71	0.72	0.61	0.79	0.80	0.79	0.80	0.81	0.81	0.82	0.75	0.75	0.75
Classification*	t.	t.	p.	t.	t.	t.	t.	t.	p.	t.	p.	p.	p.	t.	p.	p.	p.	p.
Fe/Mg	0.73	0.98	0.28	0.37	0.40	0.42	0.38	0.65	0.26	0.25	0.26	0.25	0.24	0.24	0.22	0.33	0.34	0.33

p. = pargasite; t. = tschermakite; t.h. = tschermakitio hornblende
 *On basis of 24 oxygens, according to classification of Leake (1988)

olivine tholeiite with $X_{H_2O}^Y = 0.75, 0.50, \text{ and } 0.25$; however, orthopyroxene is stable in the andesite under these same conditions and occurs in greater proportions than in the runs made with pure H_2O .

Under all conditions investigated, amphiboles in the three basalts and in the nephelinite are stable to temperatures greater than those of the vapor-saturated liquidus for the andesitic composition. The SiO_2 content of the amphiboles formed from these basalts ranges from 39.3 to 46.1 percent. Separation of the low-silica amphiboles from basaltic magmas by partial melting or fractional crystallization in the presence of water would be an effective process leading toward silica enrichment, such as proposed by Bowen (1928).

These results are also consistent with the proposal set forth by Bowen (1928) and developed in detail by Tuthill (1968) that resorption of amphiboles, for ex-

ample by crystals sinking into hotter regions of a basaltic magma, can enrich alkalis in the liquid and develop nepheline-rich compositions.

Fractionation of amphiboles, such as the one listed in Table 6, analysis 2, from a magma of andesitic composition could lead to the development of a residual liquid intermediate between quartz diorite and granodiorite (Fig. 6). This subtraction diagram suggests that when MgO has diminished to zero by removal of approximately 20 percent amphibole crystals, the liquid remaining would contain 62.8 percent SiO_2 .

The garnets formed in the Mt. Hood andesite contain about 32 percent pyrope component, 19 percent ΣFe , and 9.4 percent CaO. Fractionation of such a garnet in magmas at pressures above the breakdown of amphibole would lead to enrichment of alkalis and silica in the residual liquid. Essentially the same

TABLE 6C. Normative Compositions (C.I.P.W.) of Amphiboles in Table 6a

Norm	1	2	3	4	5	6	7	8	9	10	11	12	13
orthoclase	2.07	2.01	1.95	1.89	3.25	1.95	1.42	1.36	3.01	2.72	3.01	2.78	4.31
albite	18.36	16.25	20.14	17.56	15.48	14.41	19.80	18.96	15.15	11.22	14.31	8.28	9.37
anorthite	23.34	24.62	20.30	20.03	27.15	21.69	27.10	26.35	25.41	23.67	21.99	22.96	22.59
nepheline	--	--	--	0.66	3.17	1.54	--	--	--	9.05	3.61	6.52	4.09
leucite	--	--	--	--	--	--	--	--	--	--	--	--	--
corundum	--	--	--	--	--	--	--	--	--	--	--	--	--
diopside	13.79	16.58	19.76	24.80	15.51	25.56	9.32	12.72	17.44	19.70	18.31	21.22	21.85
wo	(7.20)	(8.69)	(10.27)	(12.89)	(8.01)	(13.40)	(4.84)	(6.58)	(9.05)	(10.42)	(9.46)	(10.96)	(11.32)
en	(5.06)	(6.32)	(6.95)	(8.69)	(5.12)	(9.76)	(3.27)	(4.28)	(5.99)	(8.14)	(6.06)	(6.99)	(7.43)
fs	(1.53)	(1.57)	(2.54)	(3.22)	(2.38)	(2.40)	(1.21)	(1.86)	(2.40)	(1.14)	(2.79)	(3.27)	(3.10)
hypersthene	10.51	6.11	7.36	--	--	--	25.30	22.57	1.70	--	--	--	--
en	(8.08)	(4.90)	(5.39)	--	--	--	(18.48)	(15.74)	(1.21)	--	--	--	--
fs	(2.43)	(1.21)	(1.97)	--	--	--	(6.82)	(6.83)	(0.49)	--	--	--	--
olivine	20.58	23.62	20.70	25.72	25.40	24.01	4.27	5.09	28.32	21.73	24.59	26.26	26.39
fo	(15.45)	(18.56)	(14.77)	(18.26)	(16.80)	(18.90)	(3.04)	(3.44)	(19.63)	(18.83)	(16.30)	(17.33)	(18.09)
fa	(5.13)	(5.06)	(5.93)	(7.46)	(8.60)	(5.11)	(1.23)	(1.65)	(8.69)	(2.90)	(8.29)	(8.93)	(8.30)
cs	--	--	--	--	--	--	--	--	--	--	--	--	--
magnetite	5.37	4.93	5.55	5.80	5.97	3.51	10.14	11.41	4.44	5.54	6.60	6.93	5.03
ilmenite	3.82	3.99	2.58	2.53	2.30	4.37	0.74	0.84	2.37	1.20	4.16	3.67	5.22

Norm	14	15	16	17	18	19	20	21	22	23	24	25
orthoclase	3.31	3.55	3.13	3.13	3.25	3.43	3.25	2.19	--	4.31	4.26	4.26
albite	15.68	15.82	0.77	3.60	8.83	11.42	12.95	1.02	--	14.81	12.21	5.32
anorthite	30.26	32.54	27.11	26.00	27.39	30.18	28.46	43.61	39.31	32.99	22.96	23.94
nepheline	1.13	--	8.98	8.78	2.51	--	--	--	2.80	--	4.16	6.83
leucite	--	--	--	--	--	--	--	--	0.05	--	--	--
corundum	--	--	--	--	--	--	--	0.51	--	--	--	--
diopside	15.76	10.54	27.93	25.42	23.63	17.74	22.83	--	16.81	11.41	21.39	27.80
wo	(8.31)	(5.57)	(14.88)	(13.51)	(12.57)	(9.27)	(11.88)	--	(8.88)	(6.01)	(11.27)	(14.63)
en	(6.31)	(4.34)	(12.29)	(10.92)	(10.26)	(6.56)	(8.07)	--	(6.84)	(4.53)	(8.54)	(11.00)
fs	(1.14)	(0.63)	(0.76)	(0.99)	(0.80)	(1.91)	(2.88)	--	(1.09)	(0.87)	(1.58)	(2.17)
hypersthene	--	3.55	--	--	--	22.89	14.39	38.33	--	8.27	--	--
en	--	(3.10)	--	--	--	(17.74)	(10.61)	(23.70)	--	(6.93)	--	--
fs	--	(0.45)	--	--	--	(5.15)	(3.78)	(14.63)	--	(1.34)	--	--
olivine	20.06	21.31	21.70	23.14	23.71	1.15	4.66	1.59	32.23	17.15	22.47	21.28
fo	(16.71)	(18.38)	(20.32)	(21.04)	(21.85)	(0.87)	(3.35)	(0.95)	(20.97)	(14.14)	(18.67)	(17.48)
fa	(3.35)	(2.93)	(1.38)	(2.10)	(1.86)	(0.28)	(1.31)	(0.64)	(3.69)	(3.01)	(3.80)	(3.80)
cs	--	--	--	--	--	--	--	--	(7.57)	--	--	--
magnetite	8.82	7.87	4.87	5.96	5.22	3.74	4.22	7.50	3.15	2.84	4.34	4.57
ilmenite	3.99	3.55	2.75	2.66	2.37	7.14	8.13	4.60	2.62	4.92	5.47	5.47

Norm	26	27	28	29	30	31	32	33	34	35	36	37
orthoclase	4.61	4.37	--	6.00	--	2.65	--	8.92	4.96	--	--	--
albite	3.74	7.79	--	--	--	--	--	1.59	0.30	--	--	--
anorthite	23.43	23.21	20.84	29.48	27.75	22.23	22.03	24.72	23.51	25.01	19.59	17.86
nepheline	8.70	7.24	12.38	9.49	10.50	10.68	11.28	8.99	11.76	13.02	15.59	16.14
leucite	--	--	5.65	2.15	6.40	4.18	5.56	--	--	6.26	4.40	4.22
corundum	--	--	--	--	--	--	--	--	--	--	--	--
diopside	23.76	20.47	26.68	18.65	23.08	28.16	26.95	22.95	25.60	22.91	17.82	25.24
wo	(12.51)	(10.73)	(14.10)	(9.88)	(12.22)	(14.91)	(14.27)	(12.16)	(13.59)	(12.03)	(9.37)	(13.43)
en	(9.39)	(7.83)	(10.97)	(7.79)	(9.58)	(11.76)	(11.25)	(9.60)	(10.94)	(8.83)	(6.96)	(10.94)
fs	(1.86)	(1.91)	(1.61)	(0.98)	(1.28)	(1.49)	(1.43)	(1.19)	(1.07)	(2.05)	(1.49)	(0.87)
hypersthene	--	--	--	--	--	--	--	--	--	--	--	--
en	--	--	--	--	--	--	--	--	--	--	--	--
fs	--	--	--	--	--	--	--	--	--	--	--	--
olivine	23.37	23.13	24.70	25.71	23.05	23.30	25.35	25.74	23.59	25.02	30.78	26.25
fo	(19.18)	(18.23)	(20.76)	(22.57)	(19.70)	(20.46)	(21.71)	(22.64)	(21.30)	(19.81)	(21.30)	(23.05)
fa	(4.19)	(4.90)	(3.34)	(3.14)	(2.90)	(2.84)	(3.04)	(3.10)	(2.29)	(5.08)	(5.01)	(2.04)
cs	--	--	(0.60)	--	(0.45)	--	(0.60)	--	--	(0.13)	(4.47)	(1.16)
magnetite	4.31	10.61	3.23	3.05	2.99	3.07	3.10	3.05	2.81	3.71	3.07	4.93
ilmenite	4.46	2.89	3.08	3.29	3.15	3.23	3.08	3.13	3.99	1.48	4.14	2.24

TABLE 7a. Composition of Quenched Liquids (Glass)

Analysis	1 ^x	2 ^x
Rock	Andesite	Andesite
T, °C	900	920
P, Kbar	13	13
Buffer	N-NO	M-H
SiO ₂	68.3	69.1
TiO ₂	0.6	0.4
Al ₂ O ₃	21.8	21.0
Fe ₂ O ₃ **	0.37	0.76
FeO	0.93	0.94
MgO	0.4	0.4
CaO	5.9	5.9
Na ₂ O	0.8	0.7
K ₂ O	0.8	0.7
Total	99.9	99.9
Mg/(Mg+ΣFe)	0.35	0.30

^xAnalyst, B.O. Mysen

**Estimate, see text.

process would work in the three basalts and the nephelinite, but the enrichment would not be as pronounced, for clinopyroxene with or without olivine would also be fractionated.

Ringwood (1974, p. 190) states that amphibole fractionation would not "greatly alter the Na/K ratio of residual liquid or partial melt" because Na/K of amphiboles and the liquids from which they crystallize are comparable. Comparison of the Na/K ratio of the starting materials (Table 1) with the amphiboles (Table 6) suggests that this is not true in all cases; most of the amphiboles in the three basalts and the nephelinite have lower Na/K than the starting materials. Ringwood (1974) also states that amphibole fractionation would not "produce the tholeiite early iron-enrichment trend," for the Fe/Mg of amphibole is comparable to the Fe/Mg of the magma. However, our data (Tables 1 and 6) show that the Fe/Mg of all but two of the amphiboles is lower than that of the starting material. Thus fractionation of these amphiboles could contribute to the tholeiitic trend of early iron enrichment.

The maximum depth to which amphiboles synthesized from these rocks can exist is about 75 to 100 km (Fig. 5). However, igneous amphiboles contain some (F⁻) in the (OH⁻) sites, and recent experimental work by Holloway and Ford (1975) reveals that F-bearing amphiboles are stable to greater pressures (and temperatures) than their hydroxy analogs. Thus, H₂O, as well as alkalis, in amphiboles from rocks of

andesitic and basaltic composition would be released by melting at these depths. Amphiboles have higher Na₂O/K₂O and lower alkali/H₂O than do micas; thus, when phlogopite or biotite forms from amphibole, excess H₂O and Na₂O will dissolve in a silicate melt. Phases such as phlogopite would remain stable to great depths, 100–175 km (Modreski and Boettcher, 1972, 1973; Forbes and Flower, 1974), before they release additional H₂O and K₂O.

It has been proposed that the K₂O content increases while K/Rb decreases in volcanic rocks across island arcs towards continental areas (Kuno, 1966; Hatherton and Dickinson, 1969; Dickinson, 1970; Jakeš and White, 1970); and similar observations have been made across the Andes (James, 1971), across the Southern California batholith (Baird, Baird, and Welday, 1974) and the central Sierra Nevada batholith (Bateman and Dodge, 1970). Partial fusion of eclogite in deeper parts of the lithosphere could contribute to these variations (Green and Ringwood, 1968). Jakeš and White (1970), Fitton (1971), and Allen *et al* (1972) also suggest that fractionation involving amphibole-liquid and mica-liquid equilibria during the partial melting of a subducting slab of oceanic crust could account for these lateral variations.

Wyllie (1973) and others have criticized our models involving amphiboles on the basis that they can play no part in the formation of magmas at distances more than 100 km from a trench because the depths would be greater than those at which amphiboles are stable (assuming a 45° dip subduction zone). Many petrologists and some geophysicists apparently are unaware that the dip of Benioff zones beneath continental areas and some island arcs is considerably less. In his original description, Benioff (1954) described these seismic zones as having three parts: (1) a shallow zone extending with flat dips under the continents to depths of about 60 km, (2) an in-

TABLE 7b. Normative Compositions (C.I.P.W.) of Liquids in Table 7a

Norm	1	2
Quartz	47.16	48.83
Orthoclase	4.73	4.14
Albite	6.77	5.92
Anorthite	29.27	29.27
Hypersthene	1.41	1.62
Fs	(0.41)	(0.62)
En	(1.00)	(1.00)
Magnetite	0.54	1.10
Ilmenite	1.14	0.76
Corundum	8.89	8.36

intermediate zone with shallow dip (22–23° under Peru and Chile) extending to 200–300 km depth, and (3) a deep zone with a dip of about 60°.

Recent evidence is that the dips of seismic zones, such as those along the continental margins of South America, are certainly small (<20°), although they are difficult to determine at depths less than about 70 km (see Isacks and Molnar, 1969; 1971; also Molnar, personal communication, 1974). In addition, the seismic zone probably does not define the upper boundary of a subducting slab at depths on the order of 70 km, but rather is *within* the slab (Isacks and Molnar, 1969). Thus, there is ample evidence that in areas of active calc-alkaline volcanism such as South America, the depths to the subduction zone may be less than 60 km. Conditions at such depths would be well within the stability ranges of our amphiboles, supporting our concept (see Boettcher, 1973) that crystal-liquid equilibria involving amphiboles is important in the genesis of the andesite-basalt clan in orogenic zones.

Acknowledgments

Conversations with Peter Molnar of the Massachusetts Institute of Technology regarding the nature of subduction zones provided valuable help. This research was supported by NSF through grants GA-12737, Ga-41203, and GY-8536 to Boettcher.

References

- ALLEN, J. C., P. J. MODRESKI, C. HAYGOOD, AND A. L. BOETTCHER (1972) The role of water in the mantle of the Earth: The stability of amphiboles and micas. *24th Int. Geol. Congr.* **2**, 231–240.
- BAIRD, A. K., K. W. BAIRD, AND E. E. WELDAY (1974) Chemical trends across Cretaceous batholithic rocks of Southern California. *Geology*, **2**, 493–495.
- BATEMAN, P. C., AND F. C. W. DODGE (1970) Variations of major chemical constituents across the Central Sierra Nevada batholith. *Geol. Soc. Am. Bull.* **81**, 409–420.
- BENCE, A. E., AND A. L. ALBEE (1968) Empirical correction factors for the electron-microanalysis of silicates and oxides. *J. Geol.* **76**, 382–403.
- BENIOFF, H. (1954) Orogenesis and deep crustal structure—additional evidence from seismology. *Geol. Soc. Am. Bull.* **65**, 385–400.
- BOETTCHER, A. L. (1973) Volcanism and orogenic belts—the origin of andesites. *Tectonophysics*, **17**, 223–240.
- , B. O. MYSEN, AND J. C. ALLEN (1973) Techniques for the control of water fugacity and oxygen fugacity for experimentation in solid-media high-pressure apparatus. *J. Geophys. Res.* **78**, 5898–5902.
- , AND P. J. WYLLIE (1968) The calcite-aragonite transition measured in the system CaO–CO₂–H₂O. *J. Geol.* **76**, 314–330.
- BOWEN, N. L. (1928) *The Evolution of the Igneous Rocks*. Princeton University Press, Princeton.
- BOYD, F. R. (1959) Hydrothermal investigations of amphiboles. In, P. Abelson, Ed., *Researches in Geochemistry*. John Wiley and Sons, Inc., New York, p. 377–396.
- , AND J. L. ENGLAND (1960) Apparatus for phase-equilibrium measurements at pressures up to 50 kilobars and temperatures up to 1750°C. *J. Geophys. Res.* **65**, 741–748.
- BULTITUDE, R. J., AND D. H. GREEN (1968) Experimental study at high pressures on the origin of olivine nephelinite and olivine melilite nephelinite magmas. *Earth Planet. Sci. Lett.* **3**, 325–337.
- , AND ——— (1971) Experimental study of crystal-liquid relationships at high pressures in olivine nephelinite and basanite compositions. *J. Petrol.* **12**, 121–147.
- BURNHAM, C. WAYNE (1967) Hydrothermal fluids at the magmatic stage. In, H. Barnes, Ed., *Geochemistry of Hydrothermal Ore Deposits*. Holt, Rinehart, and Winston, New York, p. 34–76.
- CLARK, S. P., AND A. E. RINGWOOD (1964) Density distribution and constitution of the mantle. *Rev. Geophys.* **2**, 35–88.
- DICKINSON, W. R. (1970) Relations of andesites, granites, and derivative sandstones to arc-trench tectonics. *Rev. Geophys.* **8**, 813–860.
- EGGLER, D. H. (1970) Water-saturated and undersaturated melting relations in two natural andesites (abstr.). *Geol. Soc. Am. Abstr. Progr.* **2**, 544.
- (1973) Crystallization and fractionation trends in the system andesite–H₂O–CO₂–O₂ at pressures to 10 kb. *Geol. Soc. Am. Bull.* **84**, 2517–2532.
- ESSENE, E. J., B. J. HENSEN, AND D. H. GREEN (1970) Experimental study of amphibolite and eclogite stability. *Phys. Earth Planet. Interiors*, **3**, 378–384.
- EUGSTER, H. P. (1957) Heterogeneous reactions involving oxidation and reduction at high pressures and temperatures. *J. Chem. Phys.* **26**, 1760–1761.
- FITTON, J. G. (1971) The generation of magmas in island arcs. *Earth Planet. Sci. Lett.* **11**, 63–67.
- FORBES, W. C., AND M. F. J. FLOWER (1974) Phase relations of titan-phlogopite, K₂Mg₄TiAl₂Si₈O₂₀(OH)₄: A refractory phase in the upper mantle? *Earth Planet. Sci. Lett.* **22**, 60–66.
- FUDALI, R. F. (1965) Oxygen fugacities of basaltic and andesitic magma. *Geochim. Cosmochim. Acta*, **29**, 1063–1075.
- GANGULY, J., AND R. C. NEWTON (1968) Thermal stability of chloritoid at high pressure and relatively high oxygen fugacity. *J. Petrol.* **9**, 444–466.
- GILBERT, M. C. (1969) Reconnaissance study of the stability of amphiboles at high pressure. *Carnegie Inst. Wash. Year Book*, **67**, 167–170.
- GREEN, D. H. (1970) The origin of basaltic and nephelinitic magmas. *Trans. Leicester Lit. Phil. Soc.* **64**, 28–54.
- (1971) Composition of basaltic magmas as indicators of conditions of origin: Application to oceanic volcanism. *Phil. Trans. Roy. Soc. London A*, **268**, 707–725.
- (1973) Conditions of melting of basanite magma from garnet peridotite. *Earth Planet. Sci. Lett.* **17**, 456–465.
- GREEN, T. H., AND A. E. RINGWOOD (1968) Genesis of the calcalkaline igneous rock suite. *Contrib. Mineral. Petrol.* **18**, 105–162.
- HAMILTON, D. L., C. WAYNE BURNHAM, AND E. F. OSBORN (1964) The solubility of water and effects of oxygen fugacity and water content on crystallization in mafic magmas. *J. Petrol.* **5**, 21–39.
- HATHERTON, T., AND W. R. DICKINSON (1969) The relationship between andesitic volcanism and seismicity in Indonesia, the Lesser Antilles, and other island arcs. *J. Geophys. Res.* **74**, 5301–5310.
- HILL, R. E. T., AND A. L. BOETTCHER (1970) Water in the Earth's

- mantle: Melting curves of basalt-water and basalt-water-carbon dioxide. *Science*, **167**, 980-982.
- HOLLOWAY, J. R. (1970) *Phase Relations and Compositions in the Basalt-CO₂-H₂O System at High Temperatures and Pressures*. Ph.D. Thesis, The Pennsylvania State University, University Park, Pennsylvania.
- (1971) Composition of fluid phase solutes in a basalt-H₂O-CO₂ system. *Geol. Soc. Am. Bull.* **82**, 233-238.
- (1973) The system pargasite-H₂O-CO₂: A model for melting of a hydrous mineral with a mixed-volatile fluid-I. Experimental results to 8 kbar. *Geochim. Cosmochim. Acta*, **37**, 651-666.
- , AND C. WAYNE BURNHAM (1969) Phase relations and compositions in basalt-H₂O-CO₂ under the Ni-NiO buffer at high temperatures and pressures (abstr.). *Geol. Soc. Am. Abstr. Progr.* **1**, 104-105.
- , AND ——— (1972) Melting relations of basalt with equilibrium water pressure less than total pressure. *J. Petrol.* **13**, 1-29.
- , AND C. E. FORD (1975) Fluid-absent melting of the fluorohydroxy amphibole pargasite to 35 kilobars. *Earth Planet. Sci. Lett.* **25**, 44-48.
- ISACKS, B., AND P. MOLNAR (1969) Mantle earthquake mechanisms and the sinking of the lithosphere. *Nature*, **223**, 1121-1124.
- , AND ——— (1971) Distribution of stresses in the descending lithosphere from a global survey of focal-mechanism solutions of mantle earthquakes. *Rev. Geophys. Space Phys.* **9**, 103-174.
- JAKES, P., AND A. J. R. WHITE (1970) K/Rb ratios of rocks from island arcs. *Geochim. Cosmochim. Acta*, **34**, 849-856.
- JAMES, D. E. (1971) Plate tectonic model for the evolution of the Central Andes. *Geol. Soc. Am. Bull.* **82**, 3325-3346.
- JOHANNES, W., P. M. BELL, H. K. MAO, A. L. BOETTCHER, D. W. CHIPMAN, J. F. HAYS, R. C. NEWTON, AND F. SEIFERT (1971) An interlaboratory comparison of piston-cylinder pressure calibration using the albite-breakdown reaction. *Contrib. Mineral. Petrol.* **32**, 24-38.
- KUNO, H. (1966) Lateral variation of basalt magma type across continental margins and island arcs. *Bull. Volcanol.* **29**, 195-222.
- LAMBERT, I. B., AND P. J. WYLLIE (1968) Stability of hornblende and a model for the low velocity zone. *Nature*, **219**, 1240-1241.
- LEAKE, B. E. (1968) A catalog of analyzed calciferous and subcalciferous amphiboles together with their nomenclature and associated minerals. *Geol. Soc. Am. Spec. Pap.* **68**.
- LINDSLEY, D. H., AND J. L. MUNOZ (1969) Subsolidus relations along the join hedenbergite-ferrosilite. *Am. J. Sci.* **267-A**, 295-324.
- MERRILL, R. B., AND P. J. WYLLIE (1973) Absorption of iron by platinum capsules in high pressure rock melting experiments. *Am. Mineral.* **58**, 16-20.
- MODRESKI, P. J., AND A. L. BOETTCHER (1972) The stability of phlogopite and enstatite at high pressures: A model for micas in the interior of the earth. *Am. J. Sci.* **272**, 852-869.
- , AND ——— (1973) Phase relationships of phlogopite in the system K₂O-MgO-CaO-Al₂O₃-SiO₂-H₂O to 35 kilobars: A better model for micas in the interior of the earth. *Am. J. Sci.* **273**, 385-415.
- MYSEN, B. O., AND A. L. BOETTCHER (1975a) Melting of a hydrous mantle: I. Phase relations of natural peridotite at high pressures and temperatures with controlled activities of water, carbon dioxide, and hydrogen. *J. Petrol.* **16** (in press).
- , AND ——— (1975b) Melting of a hydrous mantle: II. Geochemistry of crystals and liquids formed by anatexis of mantle peridotite at high pressures and high temperatures as a function of controlled activities of water, hydrogen, and carbon dioxide. *J. Petrol.* **16** (in press).
- RINGWOOD, A. E. (1974) The petrological evolution of island arc systems. *J. Geol. Soc. London*, **130**, 183-204.
- , I. D. MACGREGOR, AND F. R. BOYD (1964) Petrological composition of the upper mantle. *Carnegie Inst. Wash. Year Book*, **63**, 147-152.
- STERN, C. R., AND P. J. WYLLIE (1975) Effect of iron absorption by noble-metal capsules on phase boundaries in rock-melting experiments at 30 kilobars. *Am. Mineral.* **60**, 681-689.
- TUTHILL, R. L. (1968) *The Hydrothermal Behavior of Basalts in Their Melting Range at 5 Kilobars*. M. S. Thesis, The Pennsylvania State University, University Park, Pennsylvania.
- WINCHELL, H. (1947) Honolulu series, Oahu, Hawaii. *Geol. Soc. Am. Bull.* **58**, 1-48.
- WISE, W. S. (1969) Geology and petrology of the Mt. Hood area: A study of high Cascade volcanism. *Geol. Soc. Am. Bull.* **80**, 969-1006.
- WYLLIE, P. J. (1973) Experimental petrology and global tectonics—a preview. *Tectonophysics*, **17**, 189-209.
- YODER, H. S., JR., AND C. E. TILLEY (1962) Origin of basalt magmas: An experimental study of natural and synthetic rock systems. *J. Petrol.* **3**, 342-532.

Manuscript received, February 5, 1975; accepted for publication, July 7, 1975.